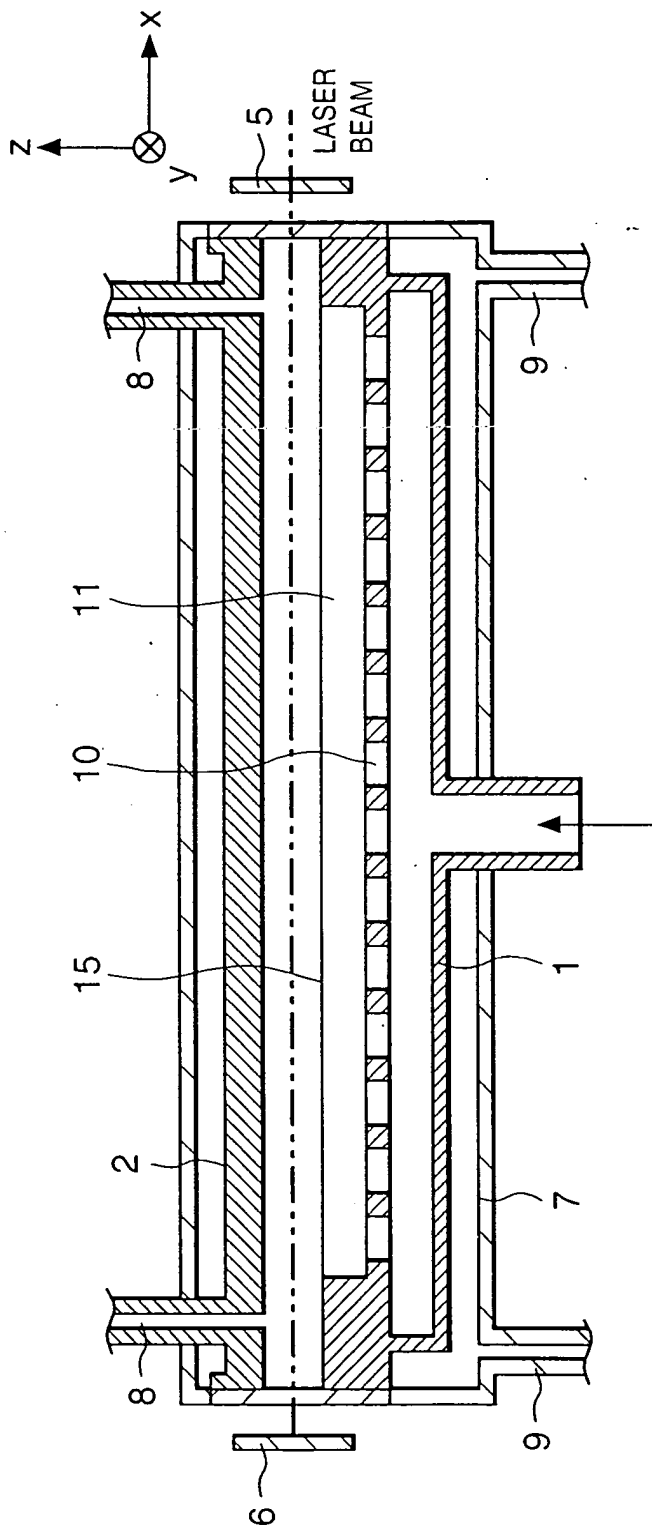


FIG. 1



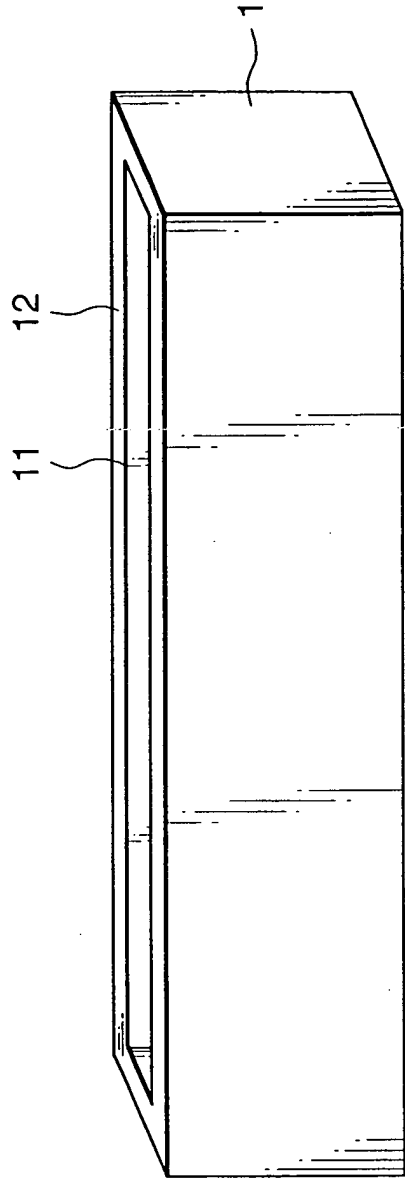


FIG. 2A

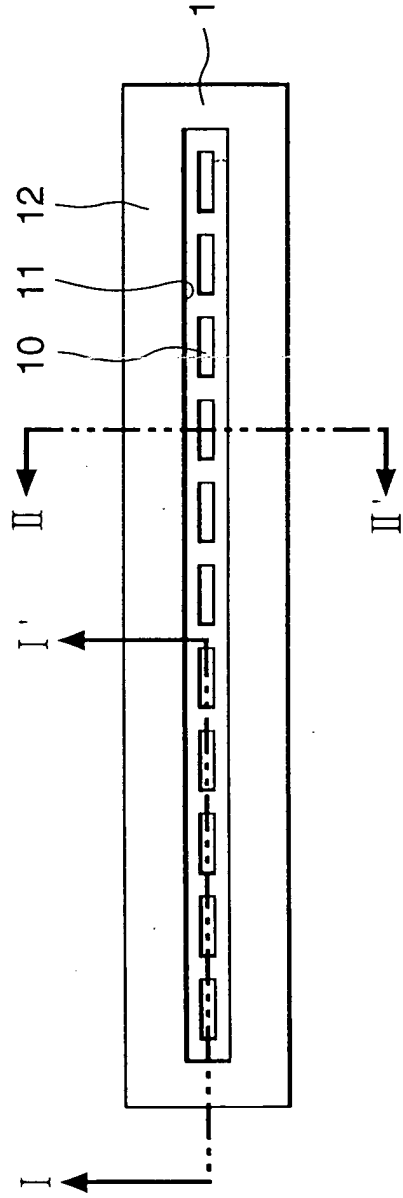


FIG. 2B

FIG. 3A

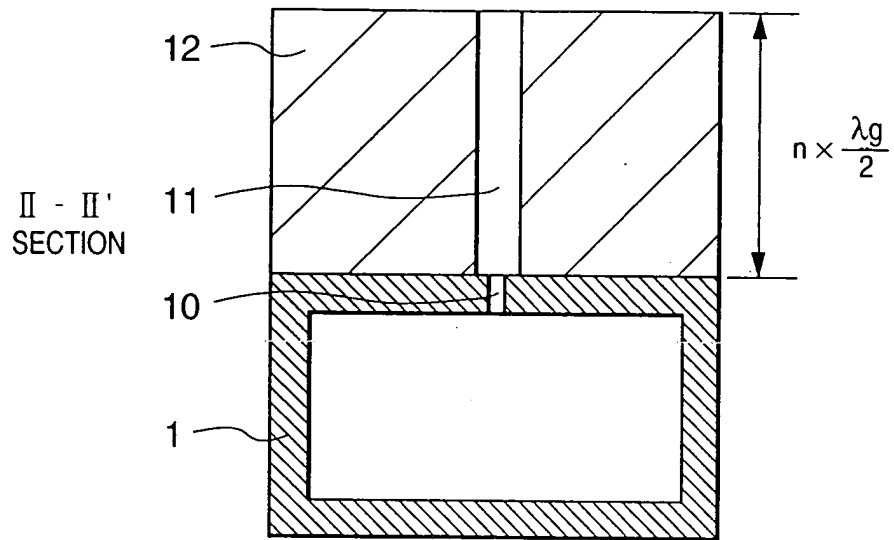


FIG. 3B

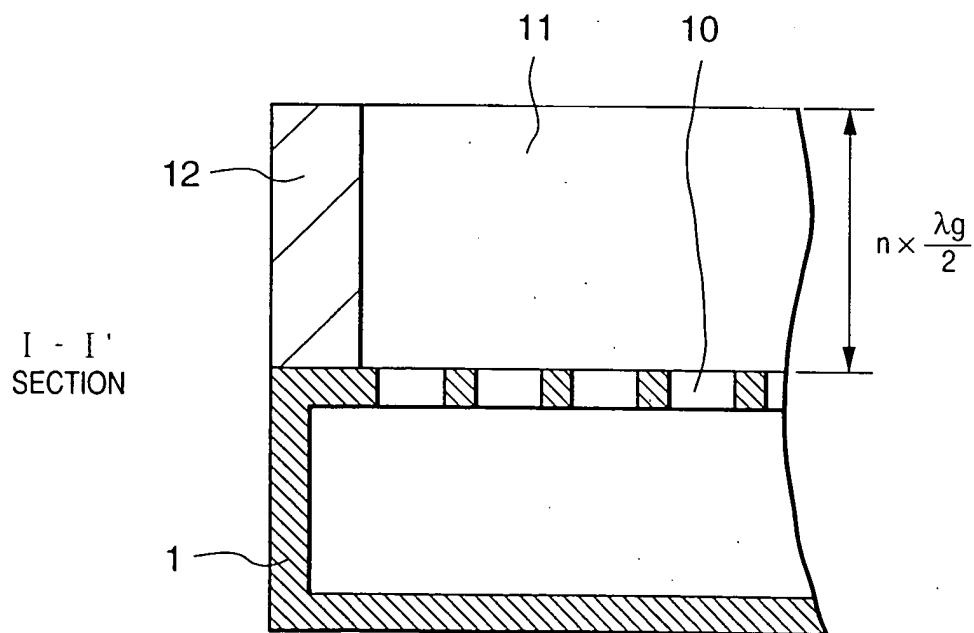


FIG. 4

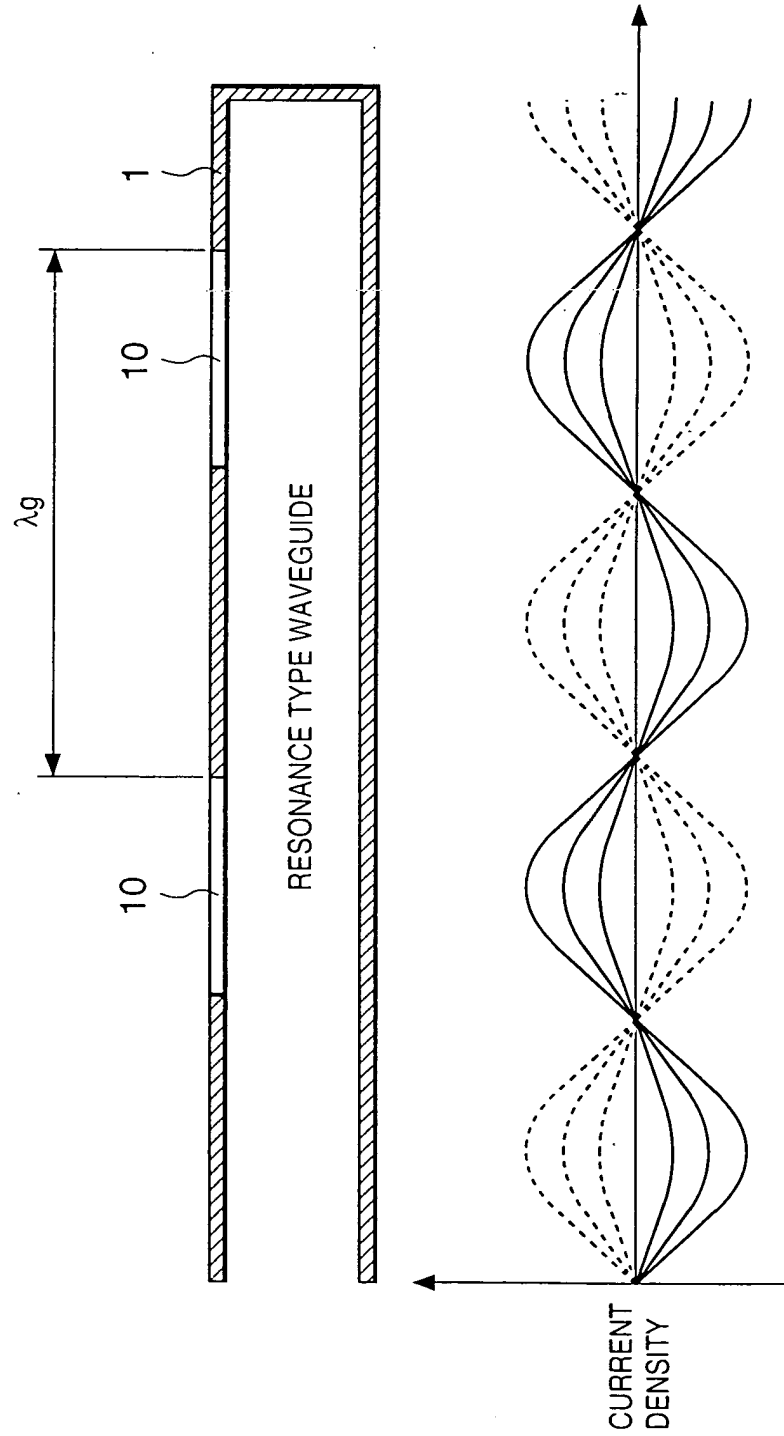


FIG. 5

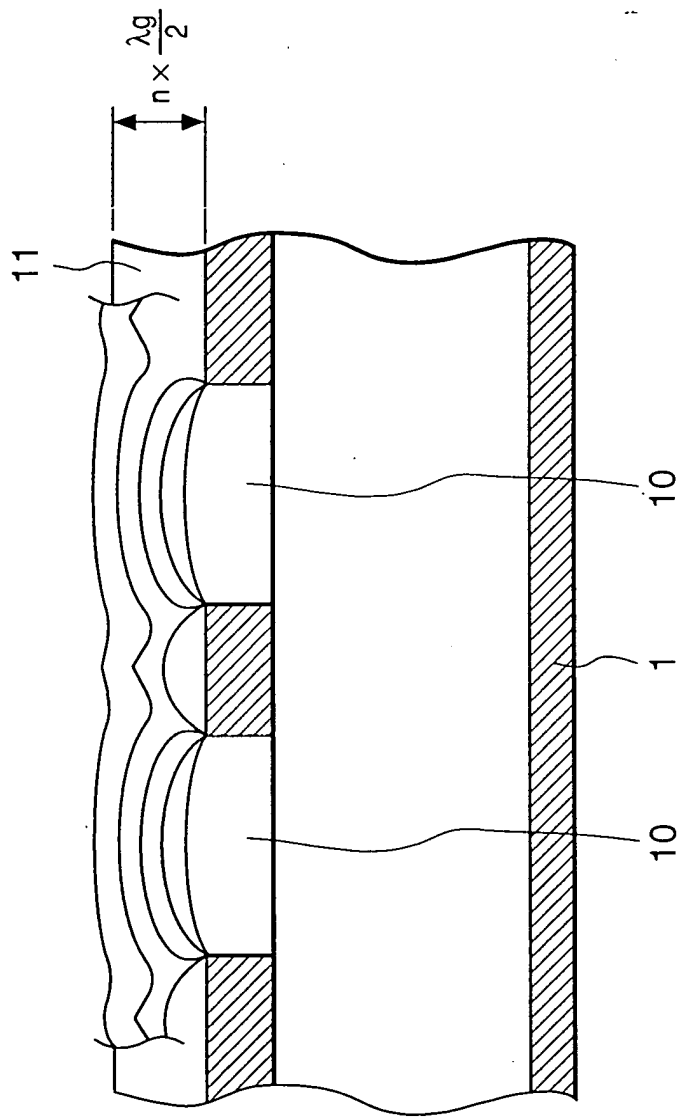


FIG. 6A

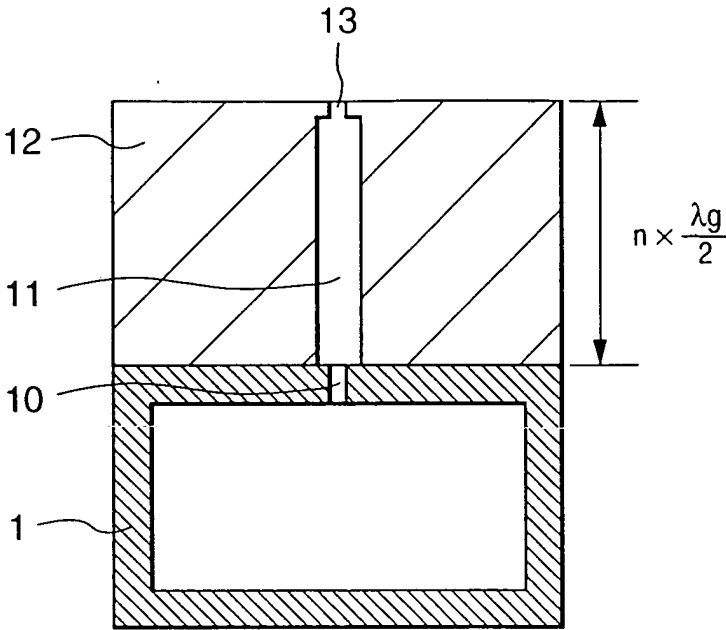


FIG. 6B

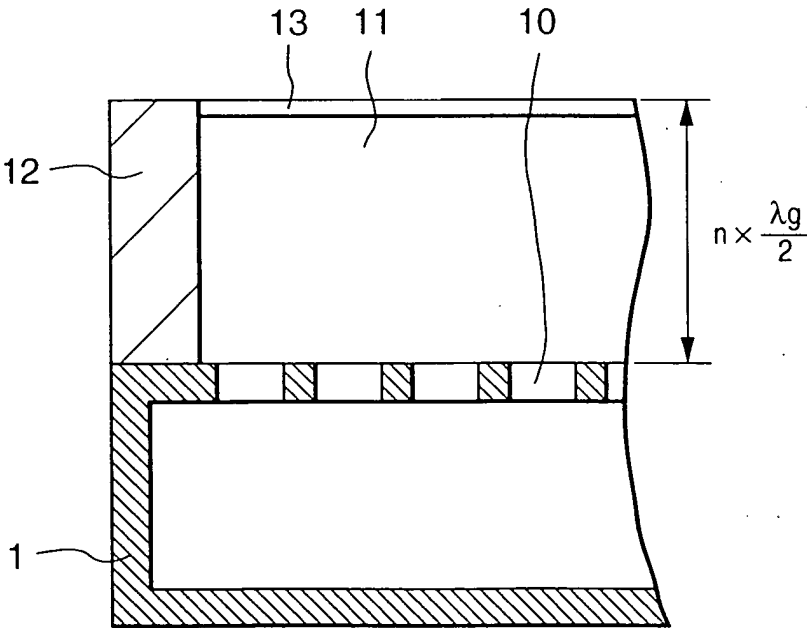


FIG. 7

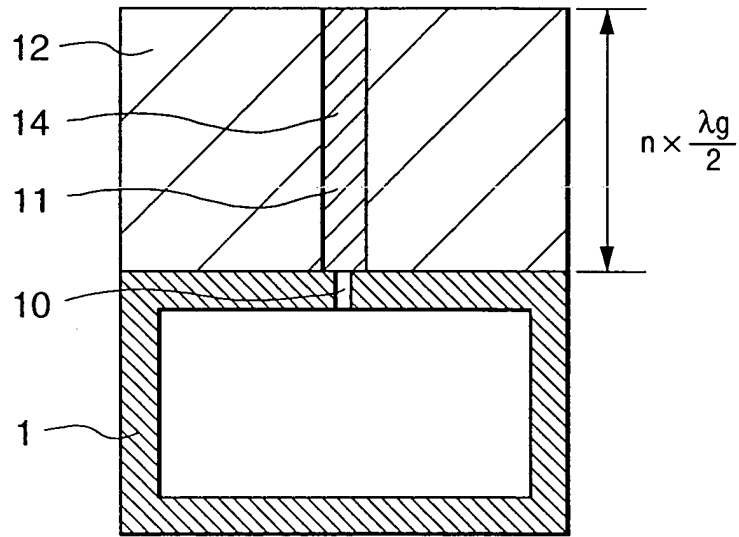


FIG. 8

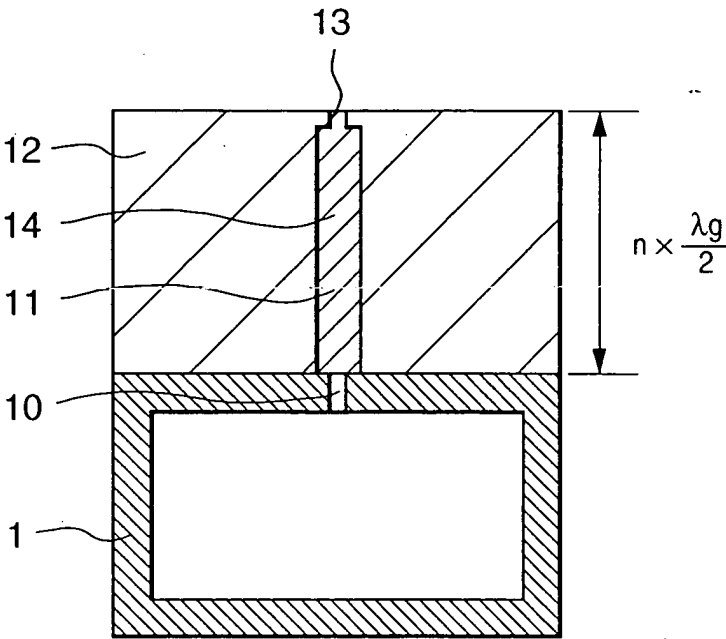


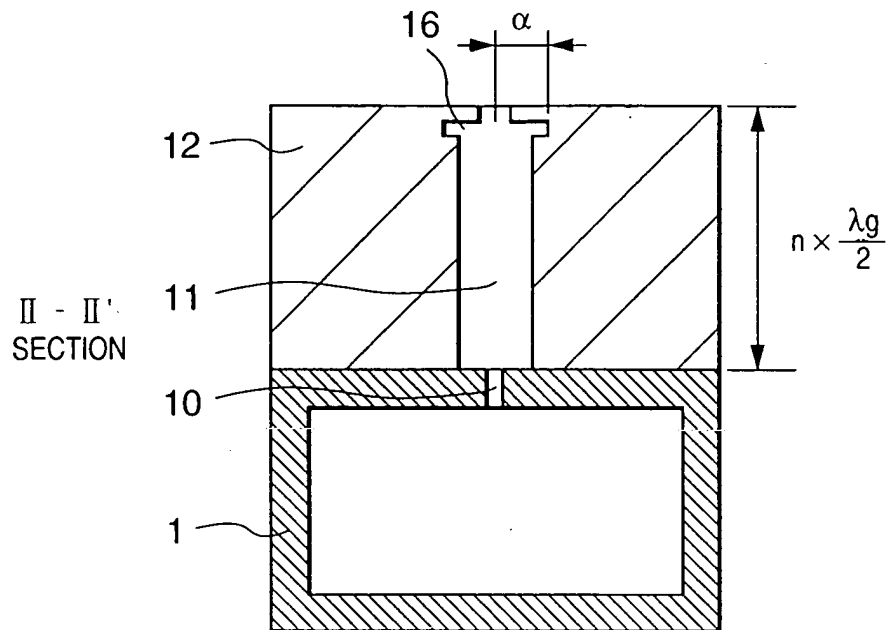
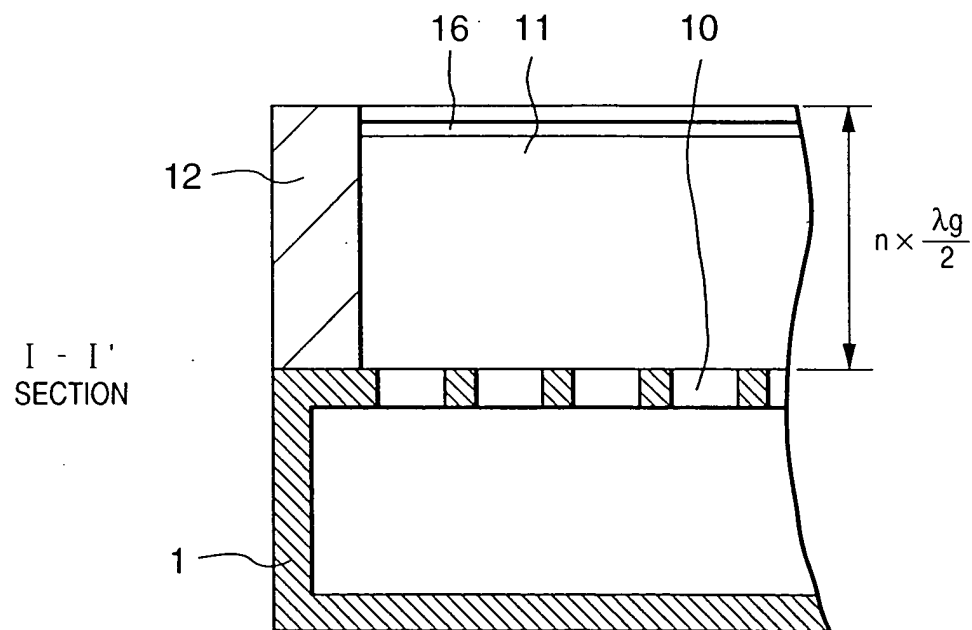
FIG. 9A**FIG. 9B**

FIG. 10

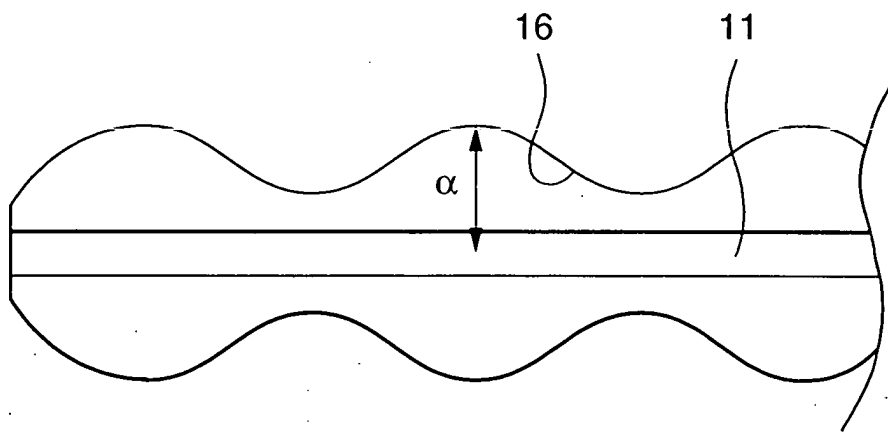
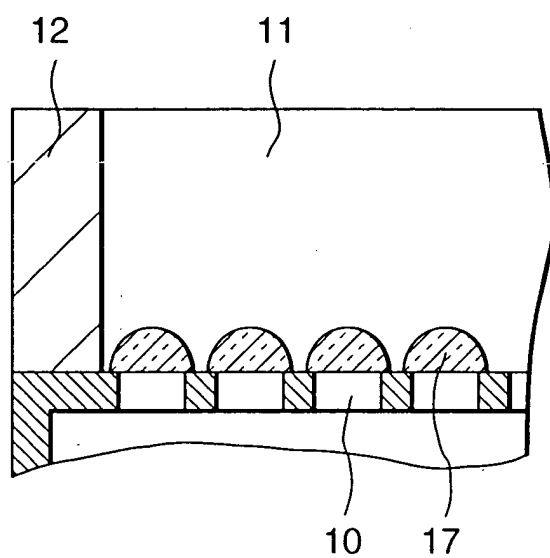


FIG. 11



001020-54546450

FIG. 12

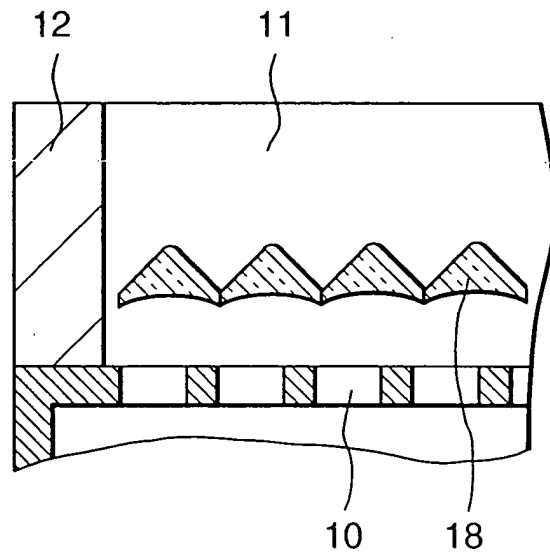


FIG. 13A

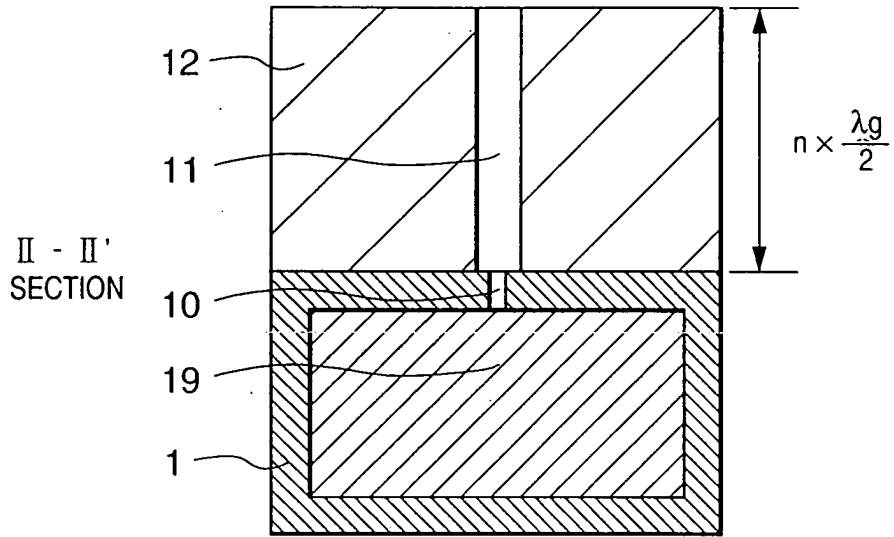


FIG. 13B

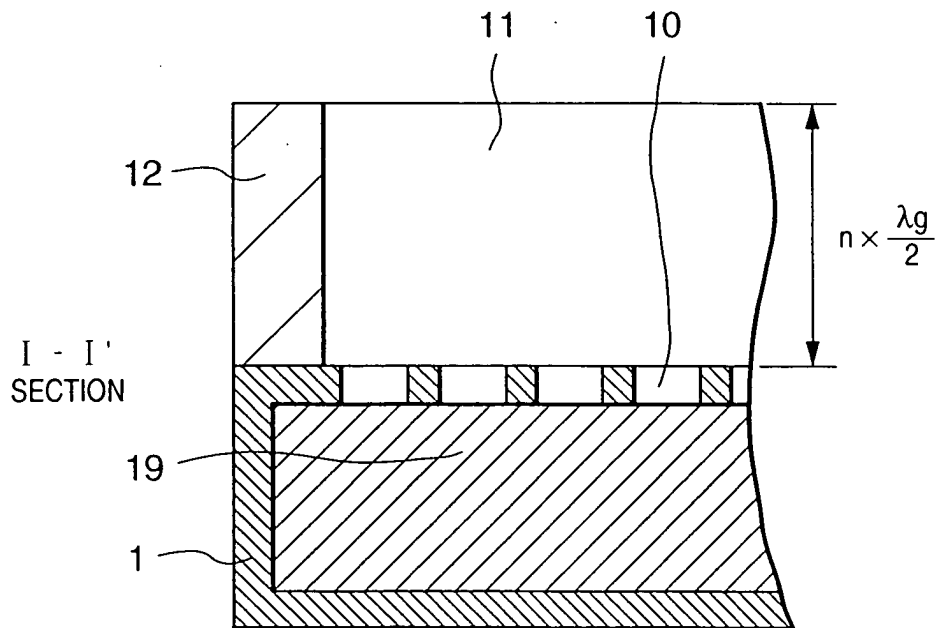


FIG. 14

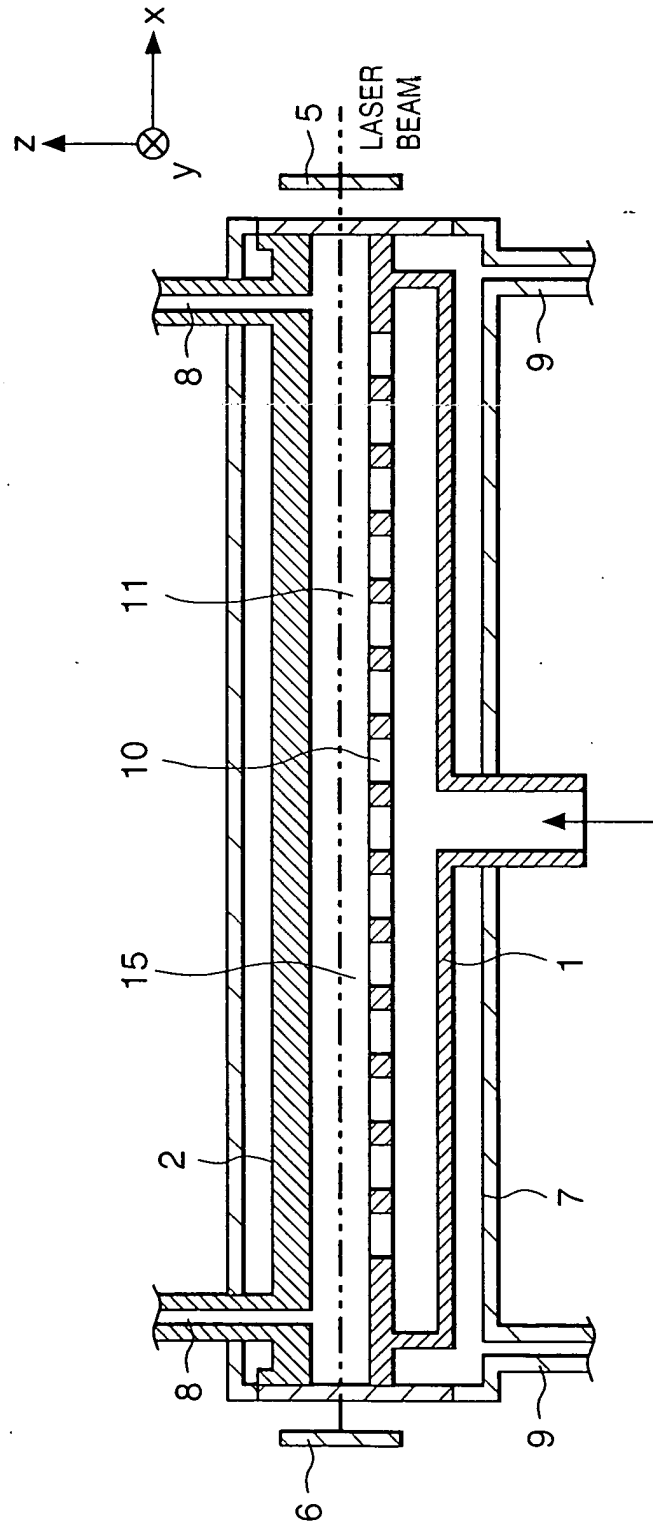


FIG. 15A

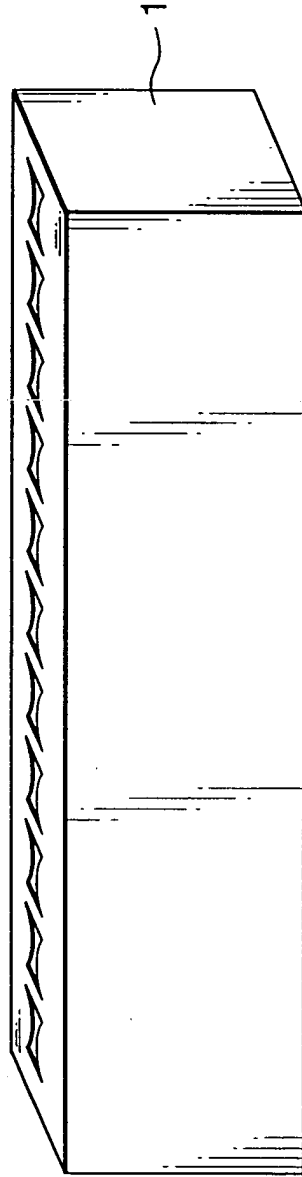


FIG. 15B

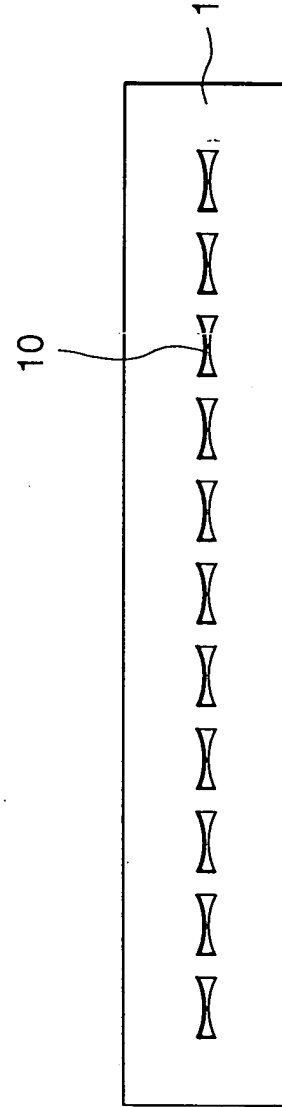


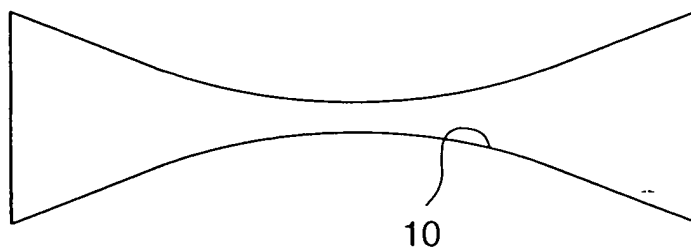
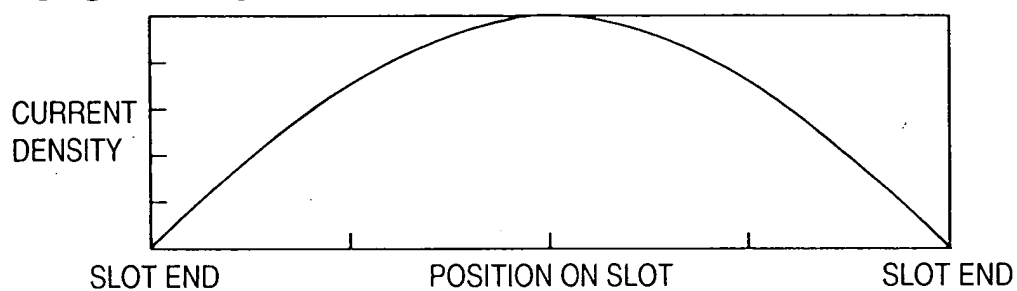
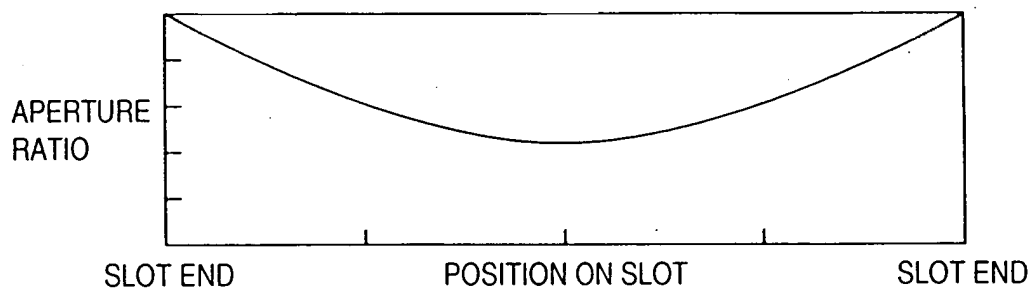
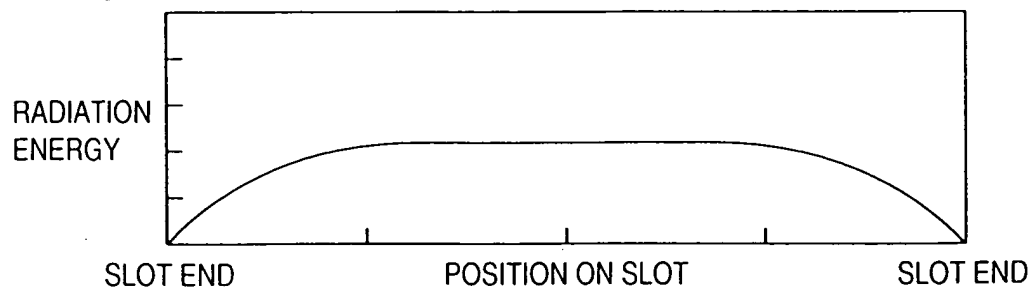
FIG. 16A**FIG. 16B****FIG. 16C****FIG. 16D**

FIG. 17A

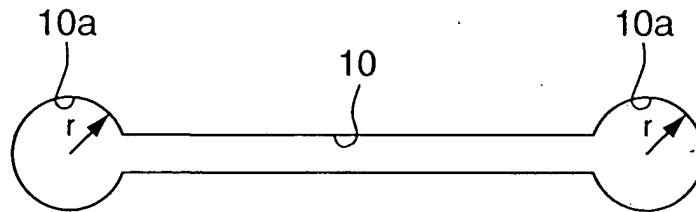


FIG. 17B

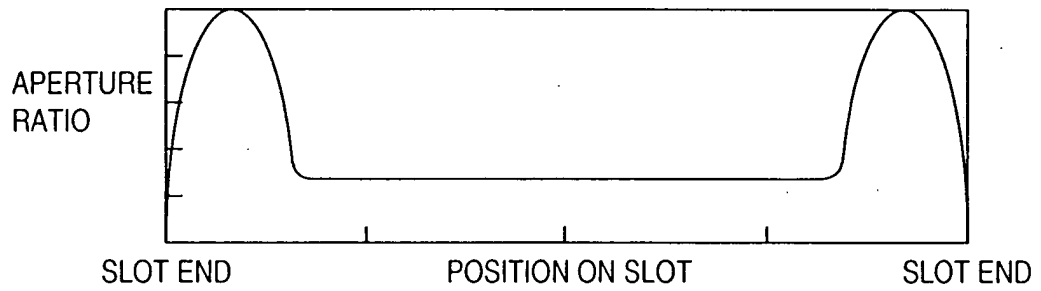


FIG. 17C

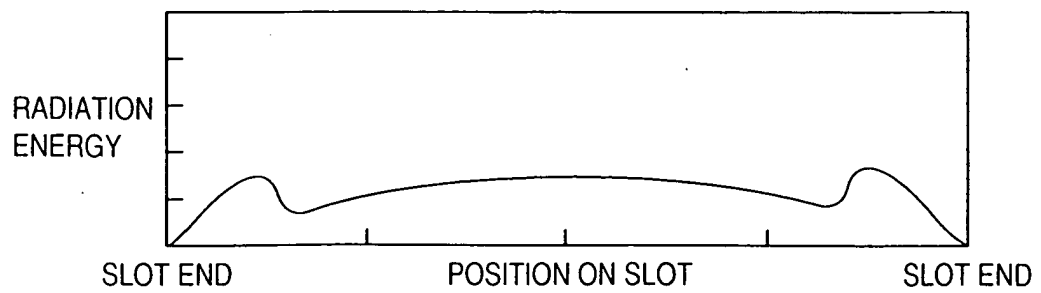


FIG. 18A

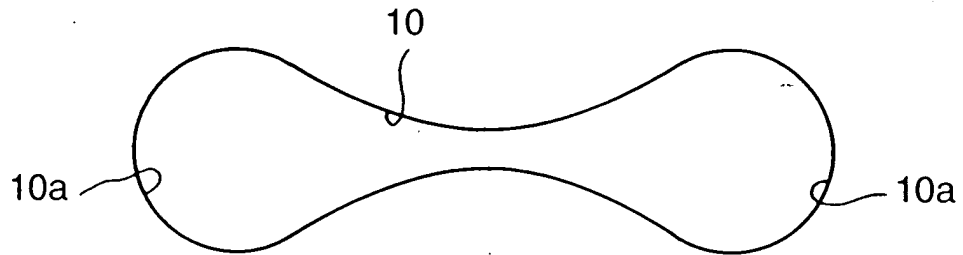


FIG. 18B

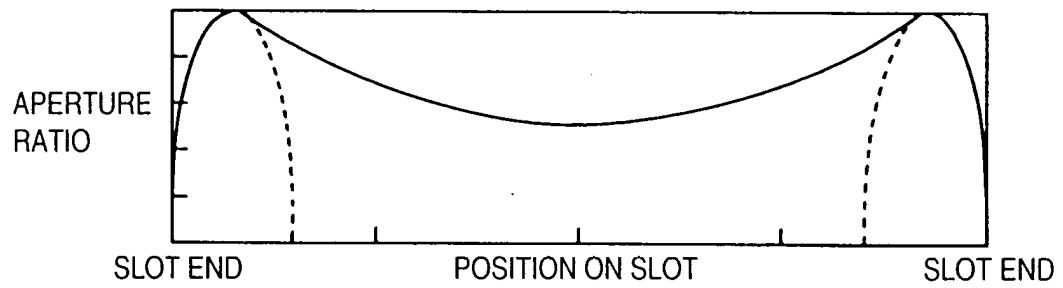


FIG. 18C

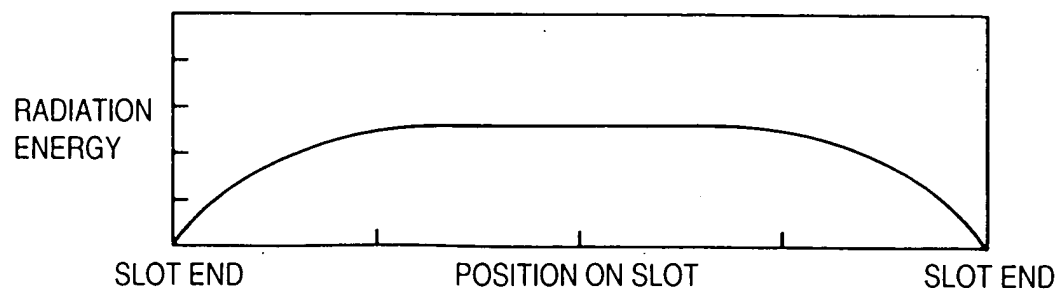


FIG. 19A

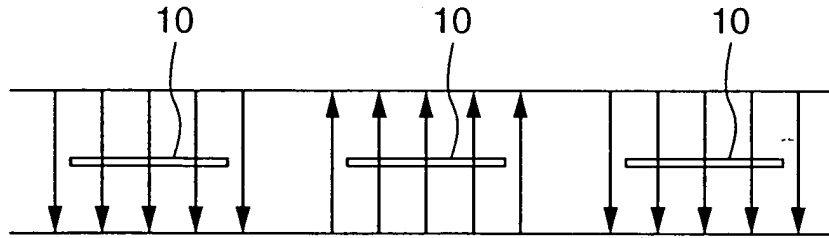


FIG. 19B

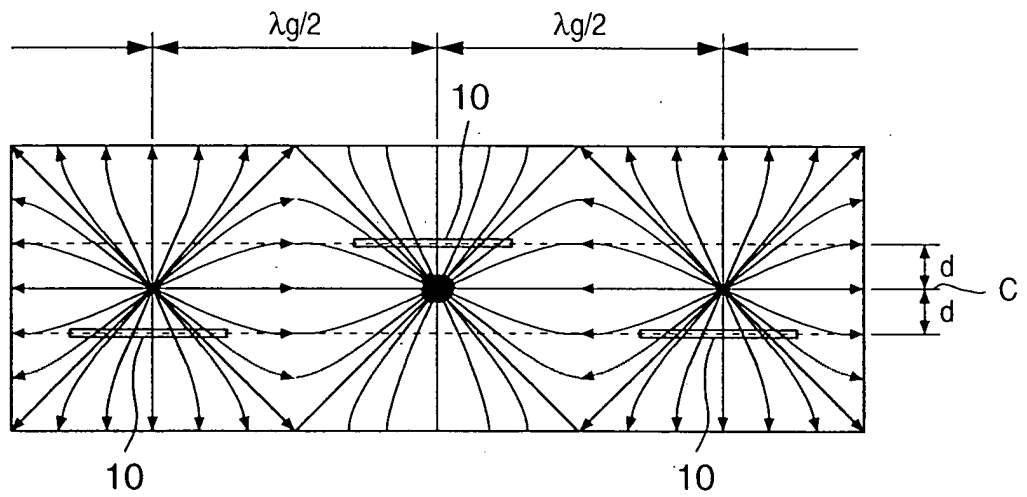


FIG. 19C

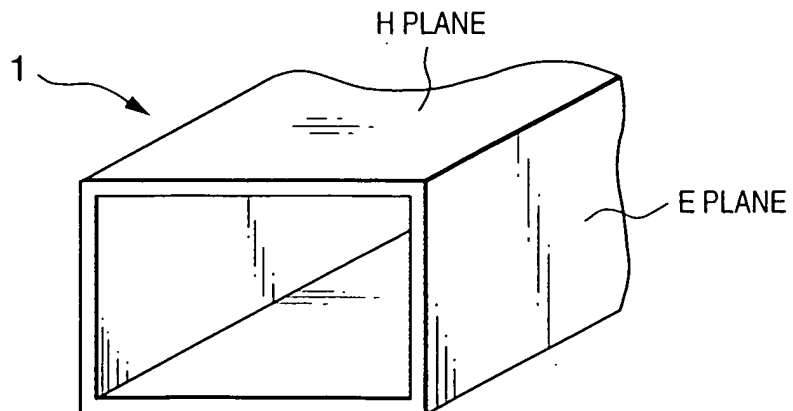


FIG. 20A

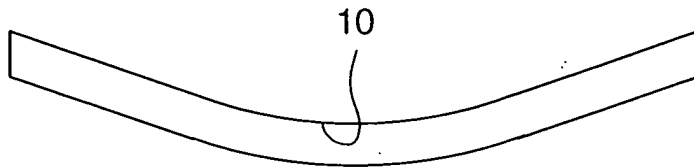


FIG. 20B

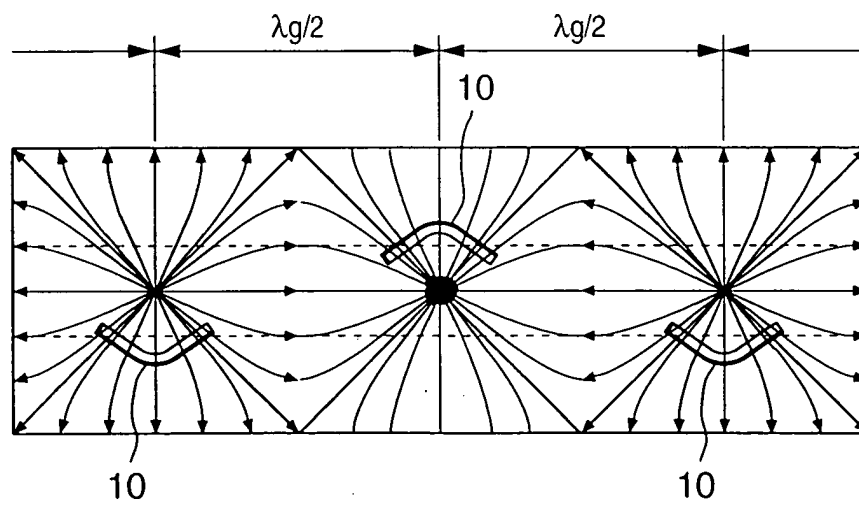


FIG. 21A

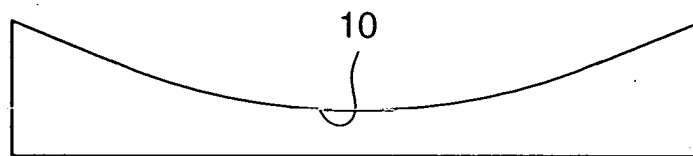


FIG. 21B

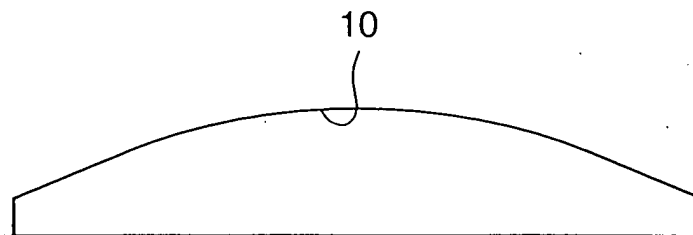


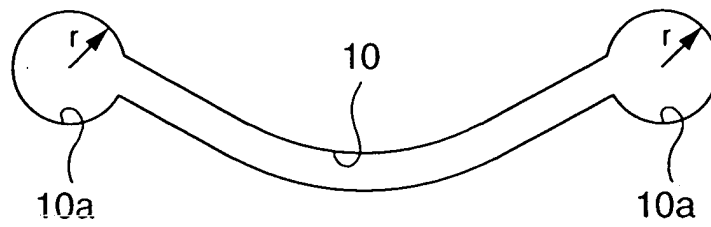
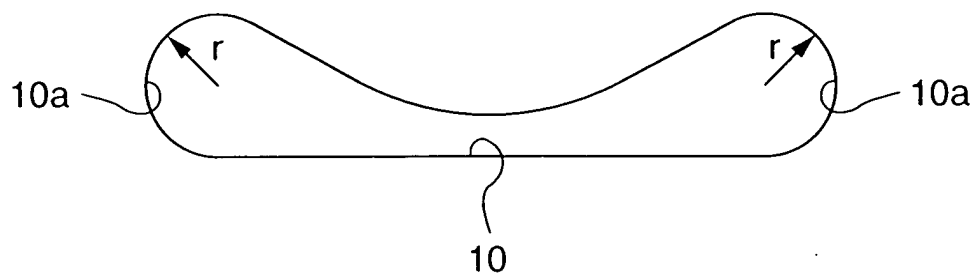
FIG. 22A**FIG. 22B**

FIG. 23

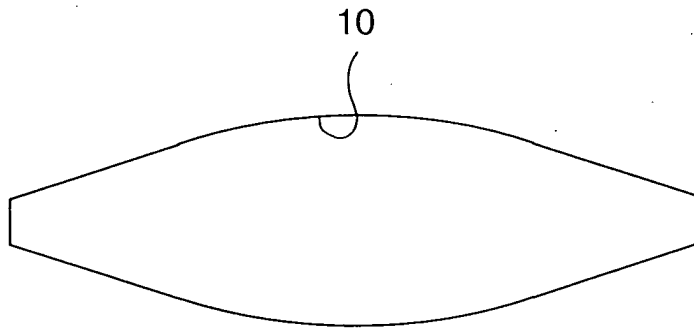


FIG. 24A

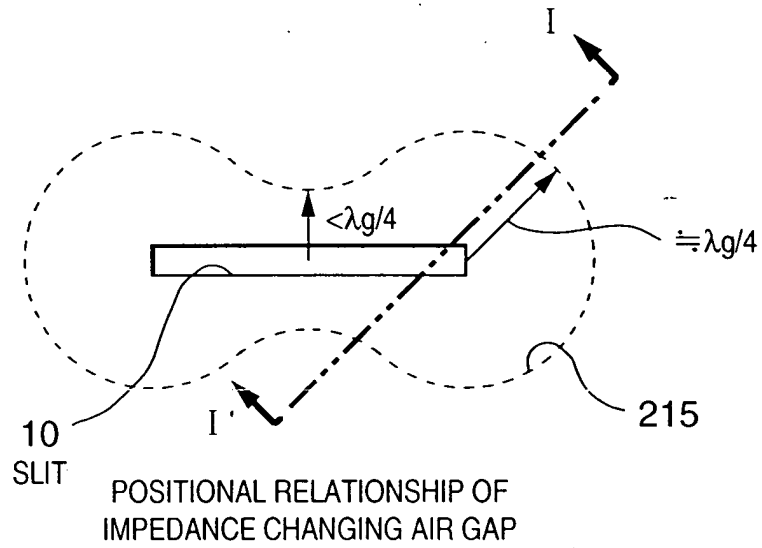
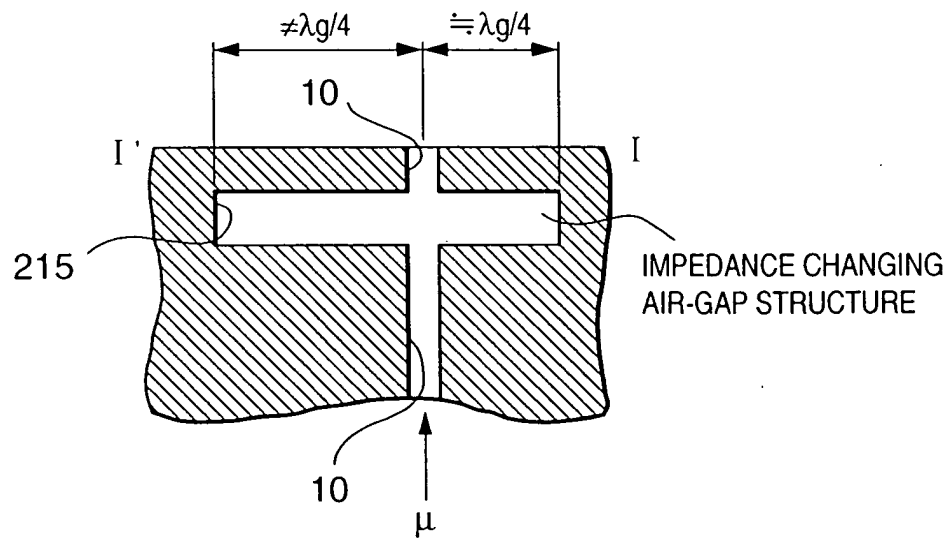


FIG. 24B



SECTIONAL VIEW (I - I') OF
IMPEDANCE CHANGING AIR GAP

FIG. 25A

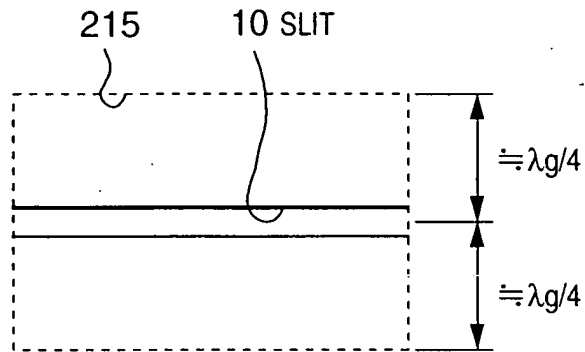
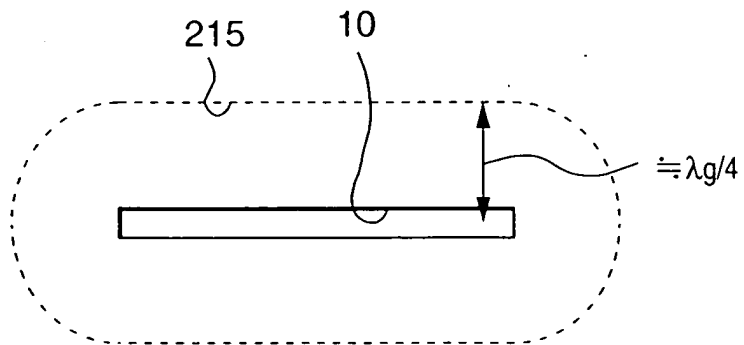


FIG. 25B



POSITIONAL RELATIONSHIP OF
 $\lambda g/4$ -LONG AIR-GAP STRUCTURE

FIG. 26A

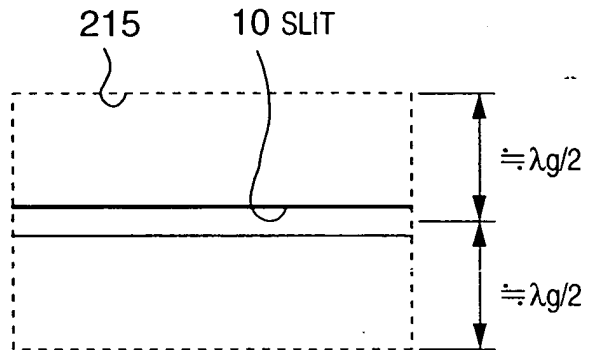
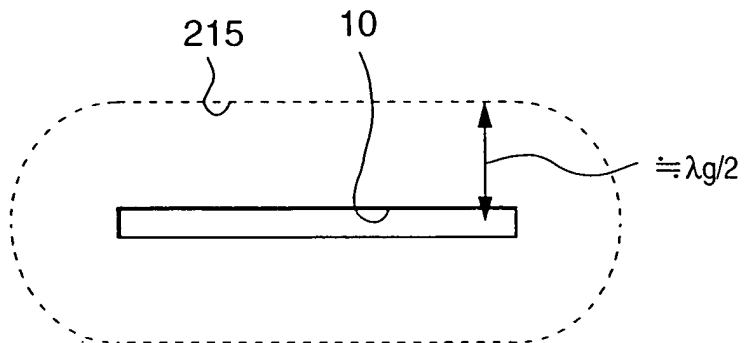
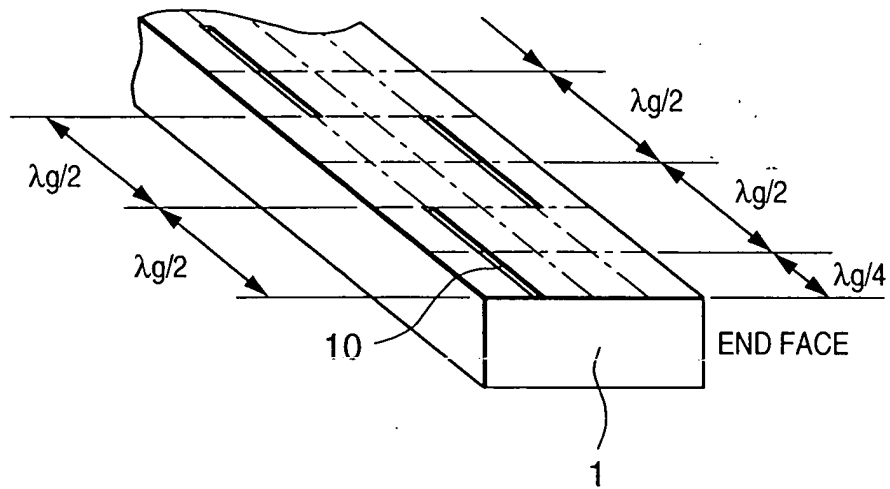


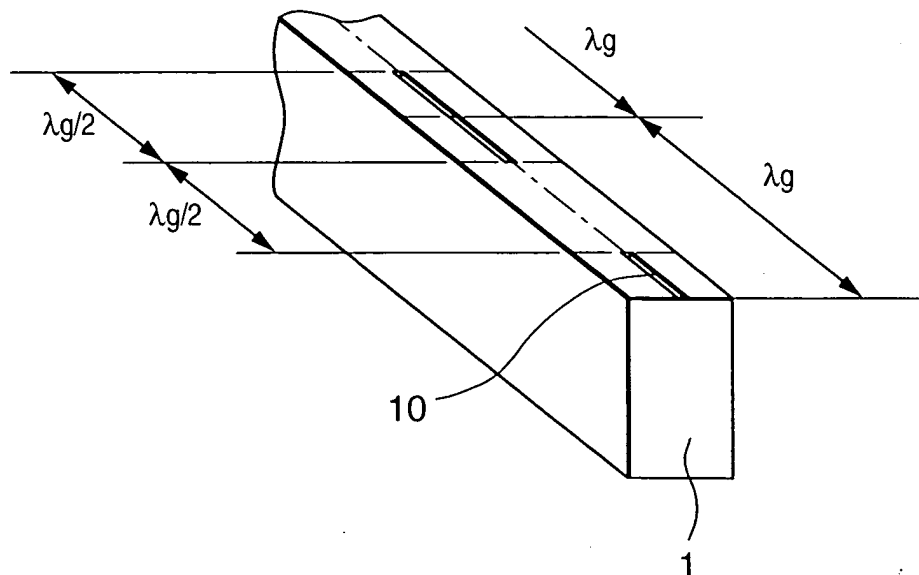
FIG. 26B



POSITIONAL RELATIONSHIP OF
 $\lambda_g/2$ -LONG AIR-GAP STRUCTURE

FIG. 27A

RESONANCE LENGTH SLOT $\lambda_g/2$ -PITCH
H-PLANE ANTENNA STRUCTURE

FIG. 27B

RESONANCE LENGTH SLOT λ_g -PITCH
E-PLANE ANTENNA STRUCTURE

28/57

FIG. 28A

TAPERED SLOT

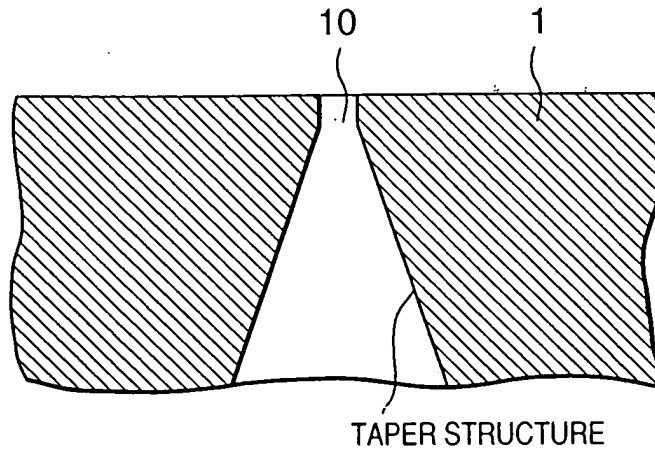


FIG. 28B

TAPERED SLOT

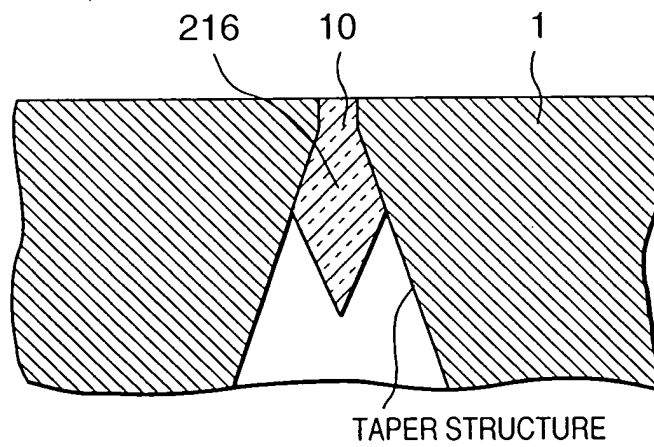


FIG. 28C

SLOT WITH LENS

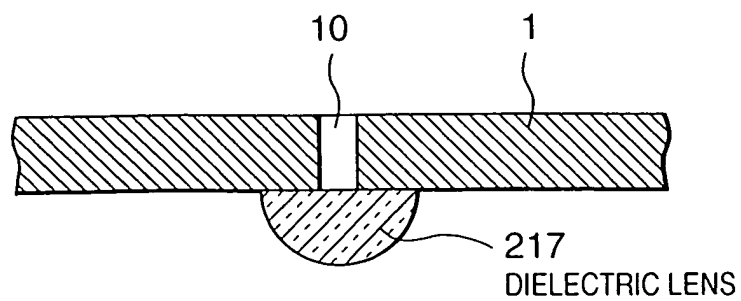


FIG. 29

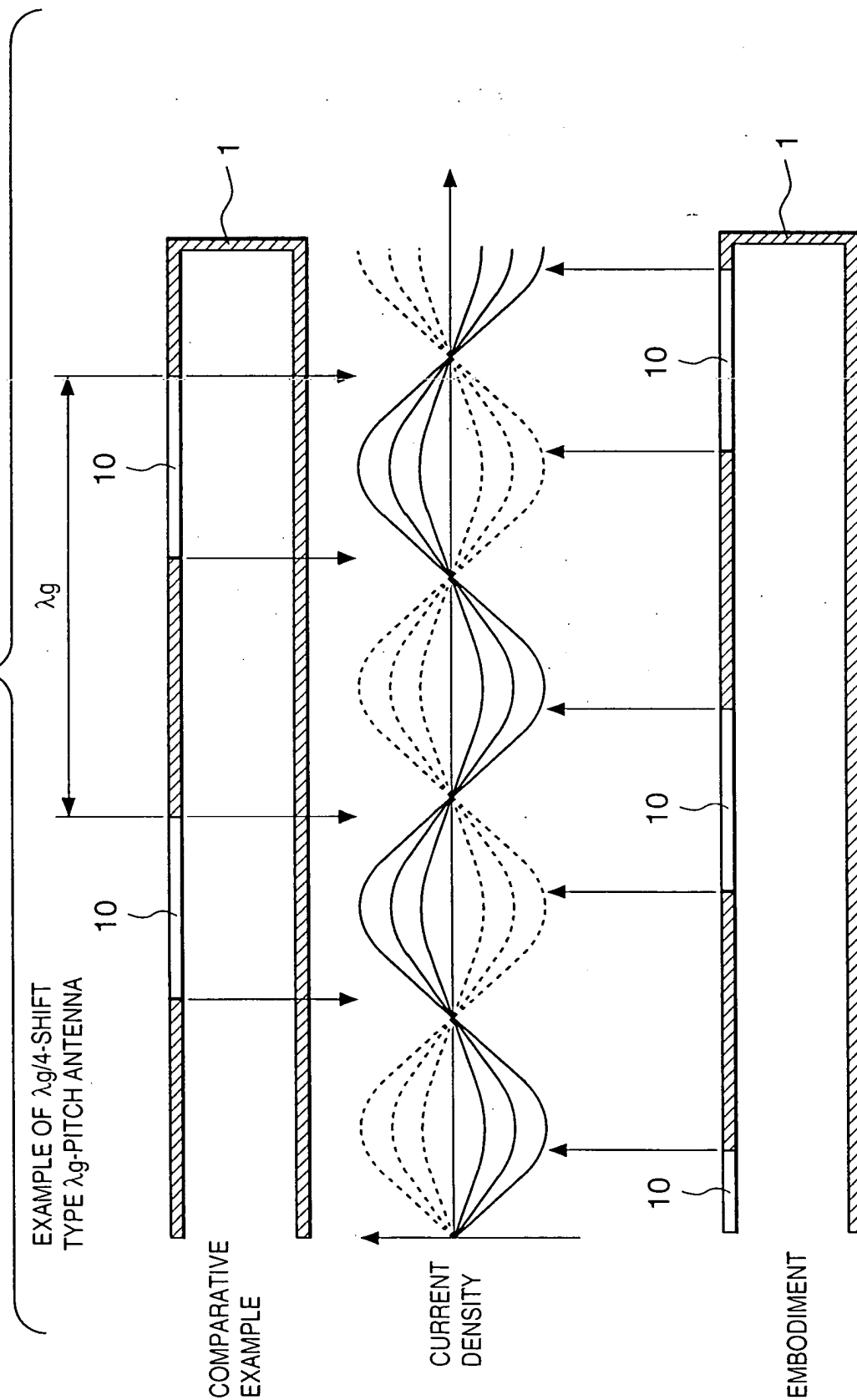


FIG. 30

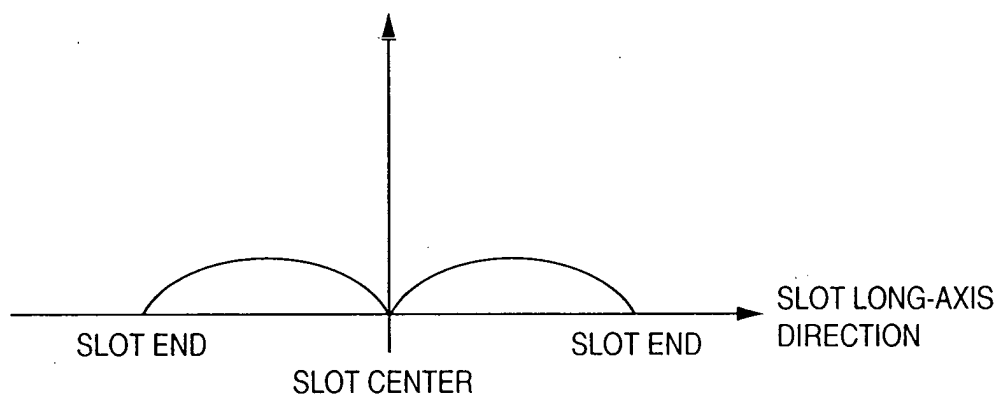
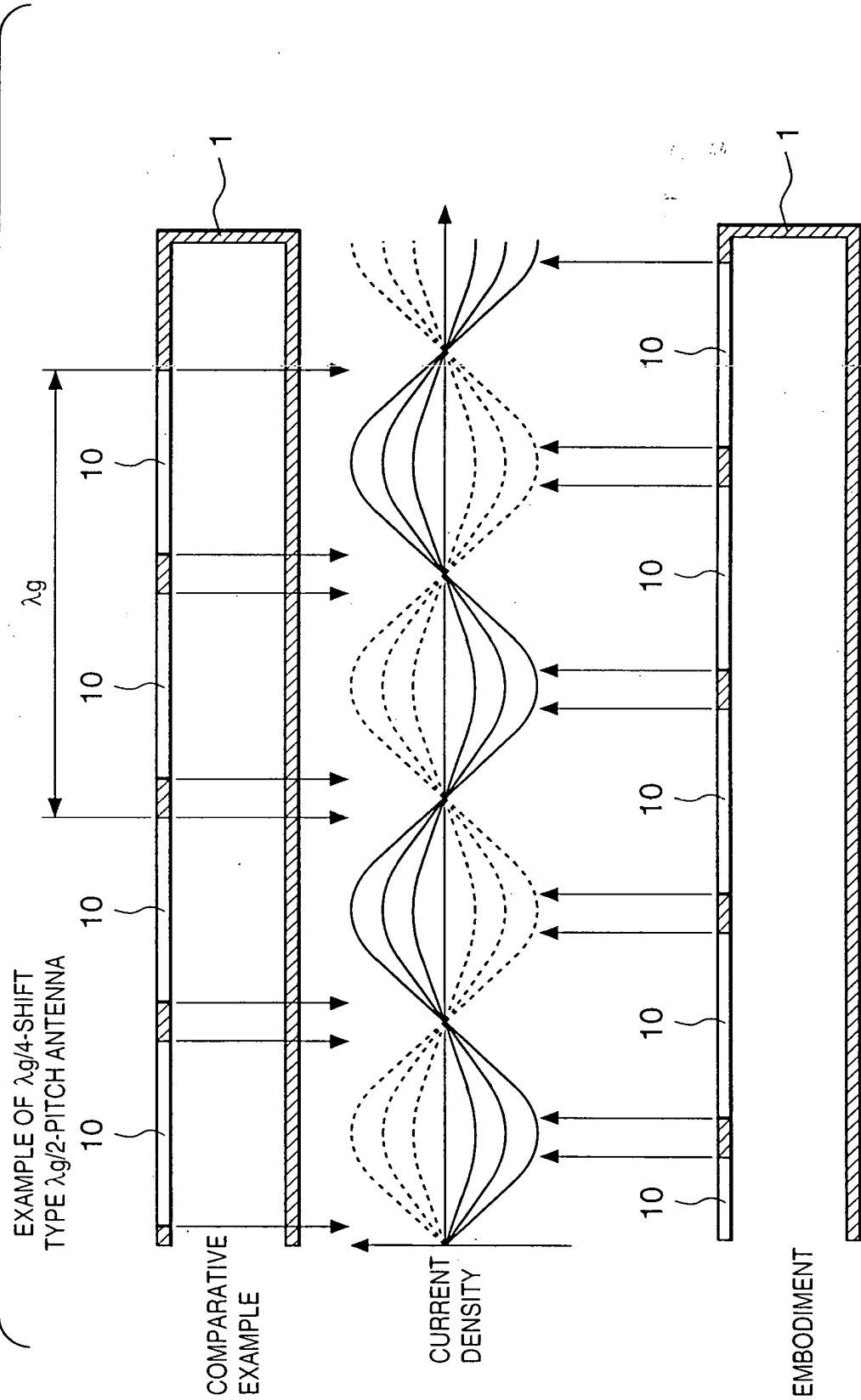


FIG. 31



EMBODIMENT

FIG. 32B

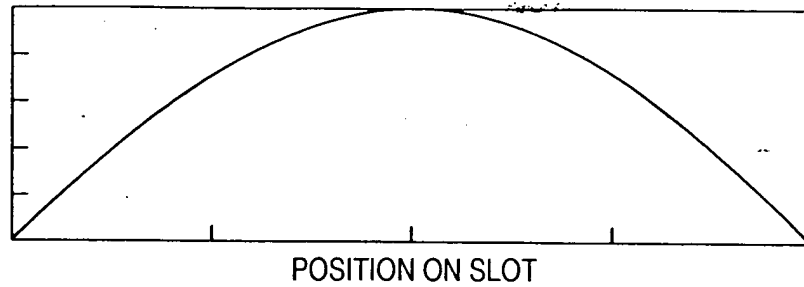


FIG. 32B

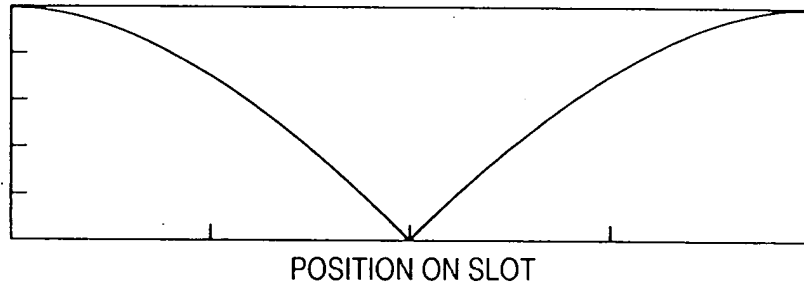
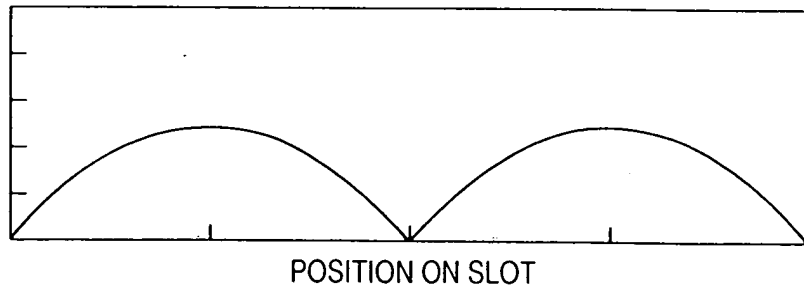


FIG. 32C



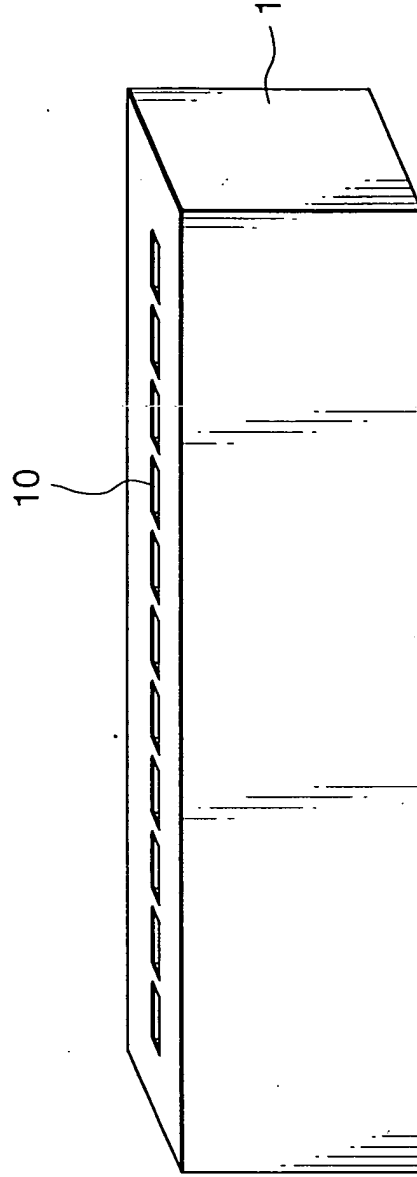


FIG. 33A

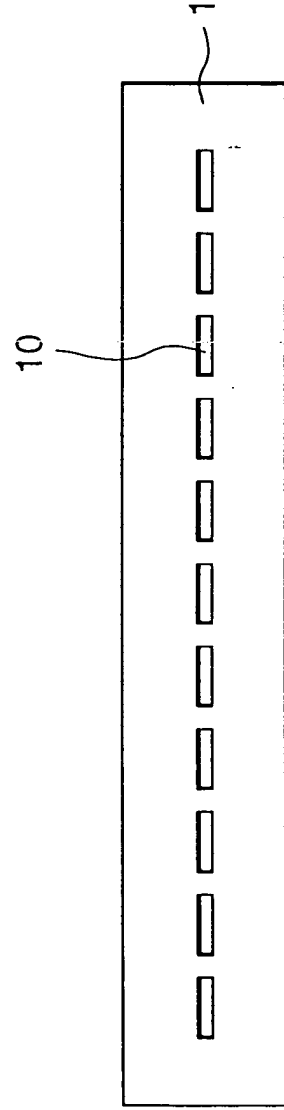


FIG. 33B

FIG. 34A

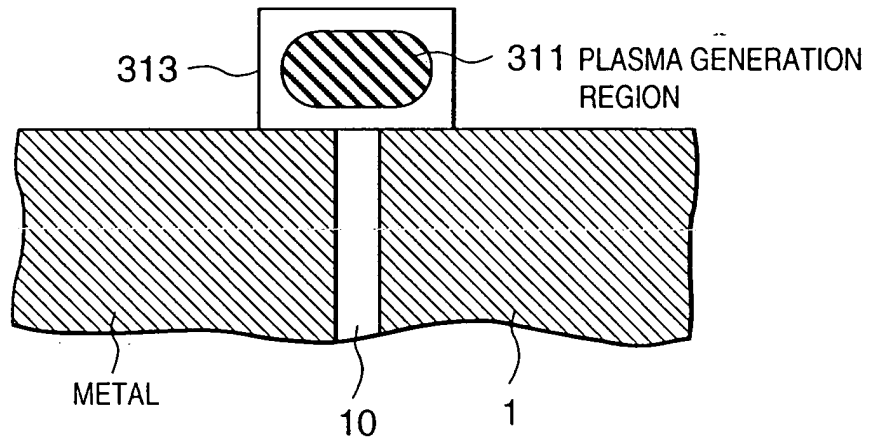


FIG. 34B

SECTION VIEWED IN DIRECTION
PERPENDICULAR TO SLOT LONG-AXIS DIRECTION

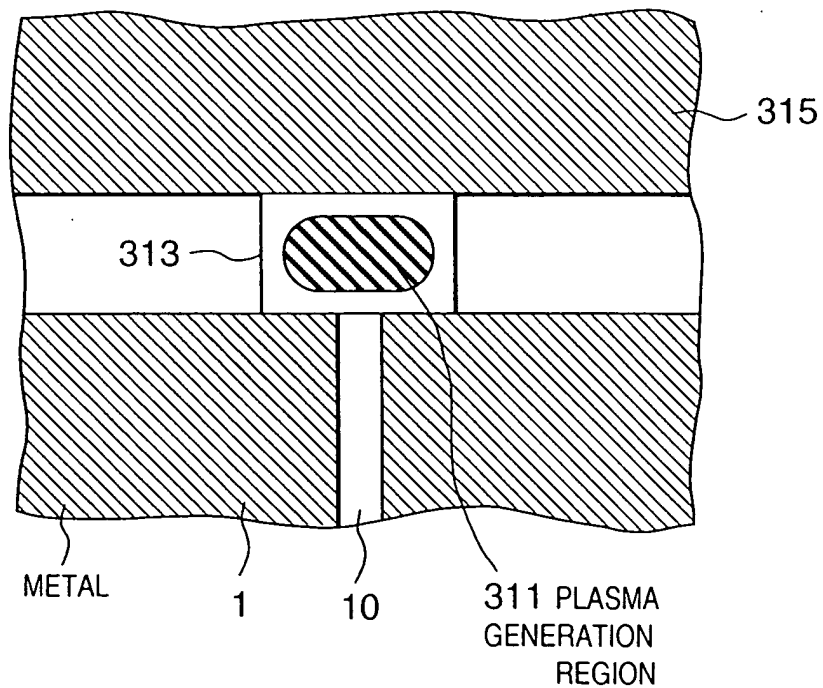
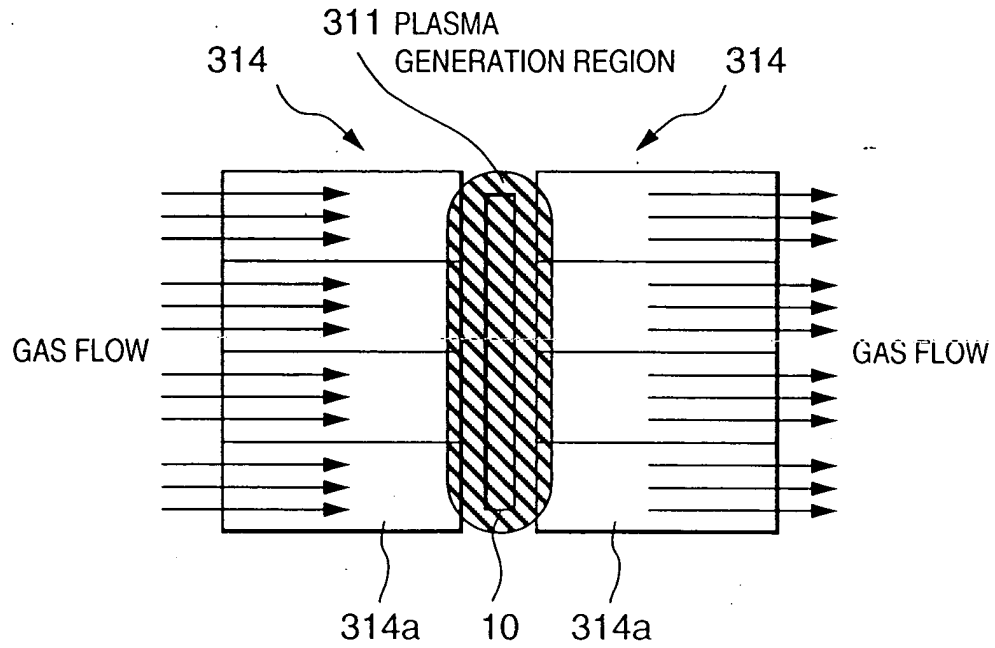


FIG. 35A

PLAN VIEW OF NOZZLE SHIELD

**FIG. 35B**

OUTLINE OF NOZZLE SHIELD

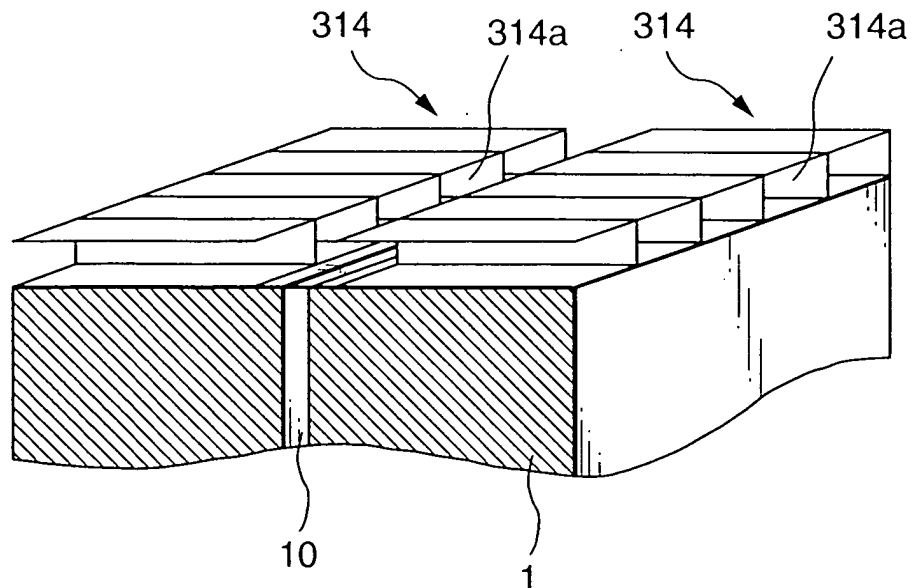


FIG. 36A

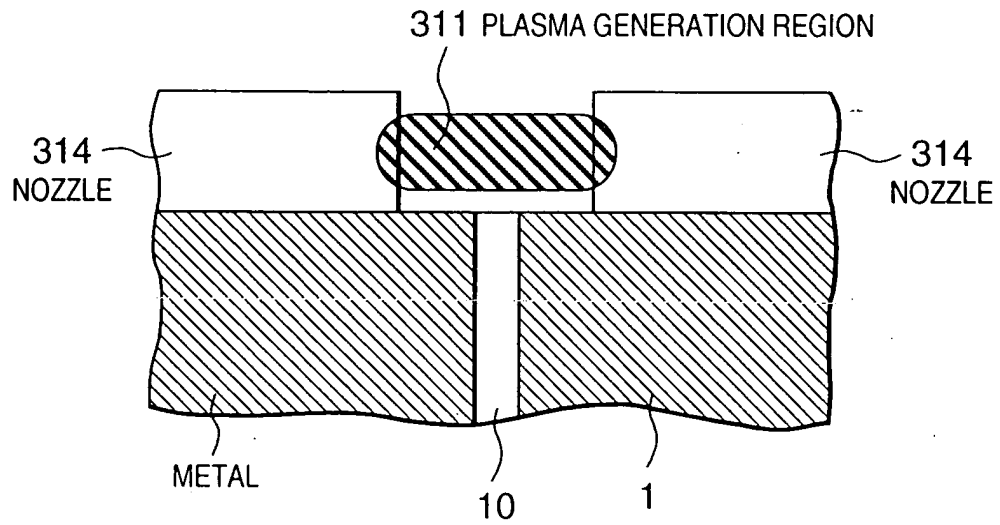


FIG. 36B

SECTION VIEWED IN SLOT
SHORT-AXIS DIRECTION

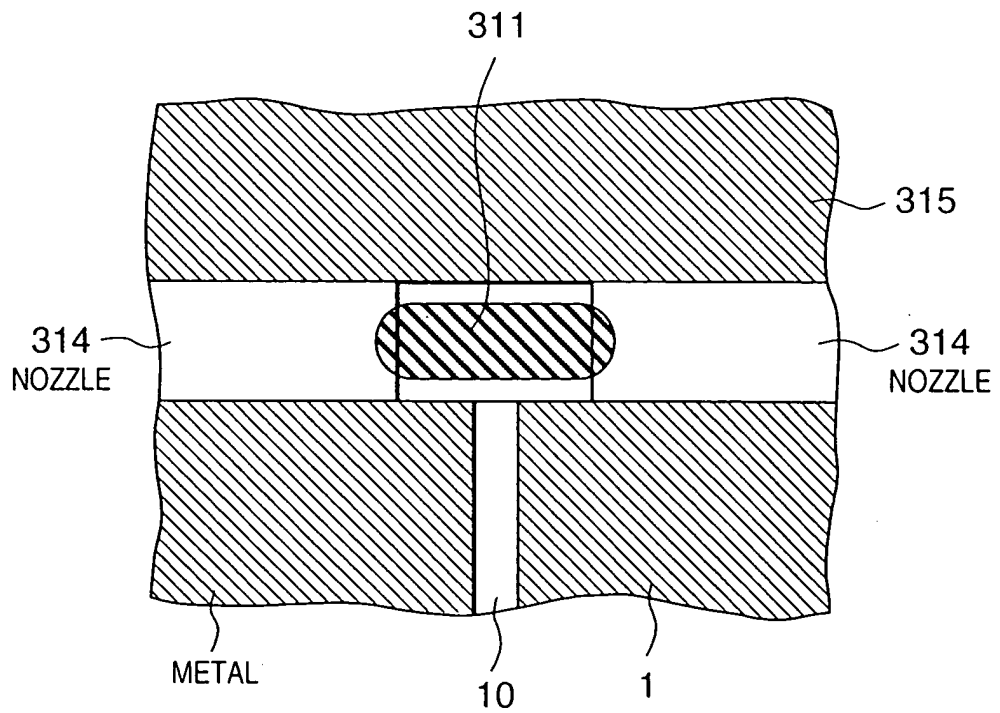


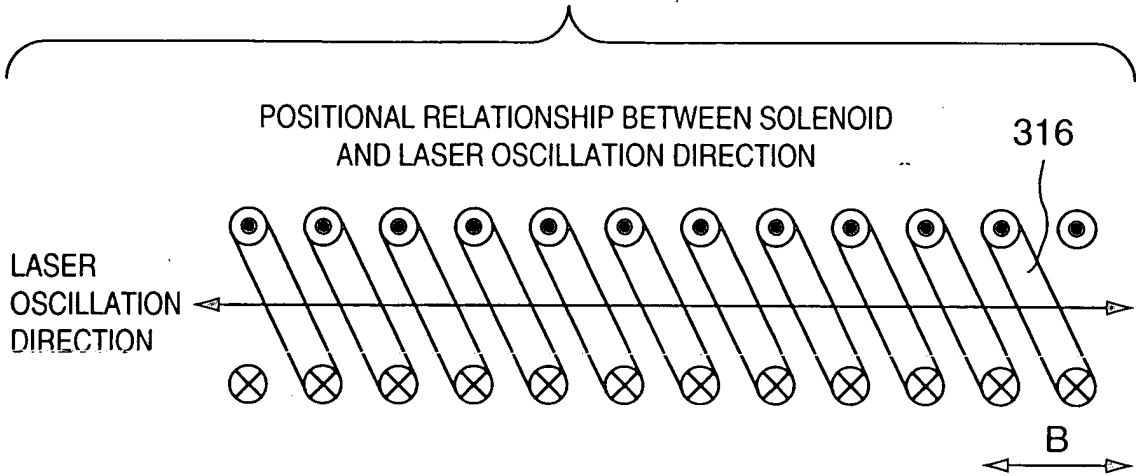
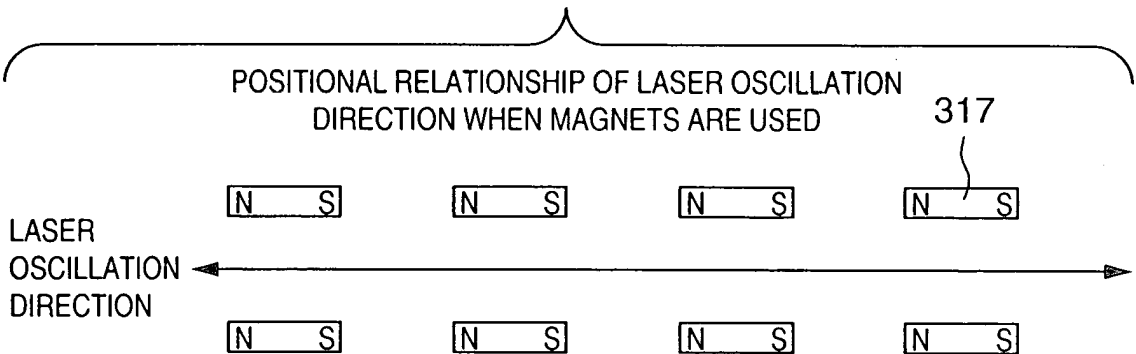
FIG. 37A**FIG. 37B**

FIG. 38A

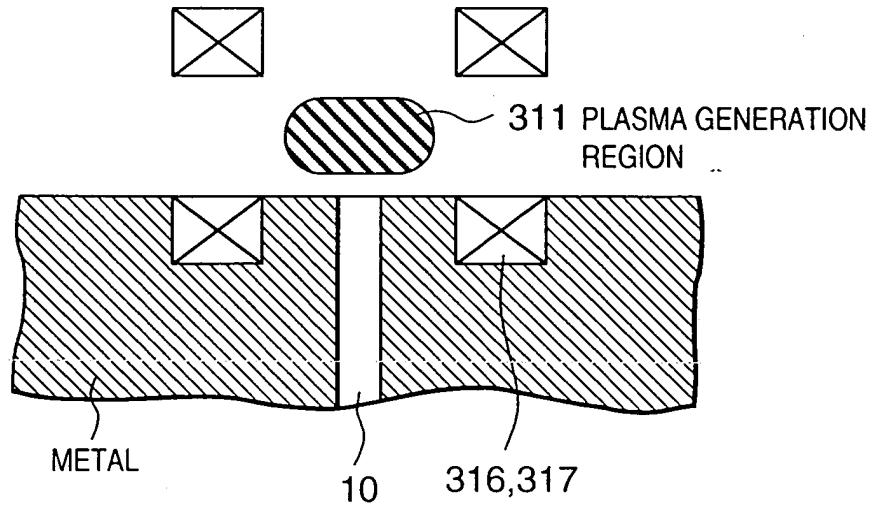


FIG. 38B

SECTION VIEWED IN SLOT SHORT-AXIS DIRECTION
(DIRECTION OF MAGNETIC FIELD IS
PERPENDICULAR TO PAPER SURFACE)

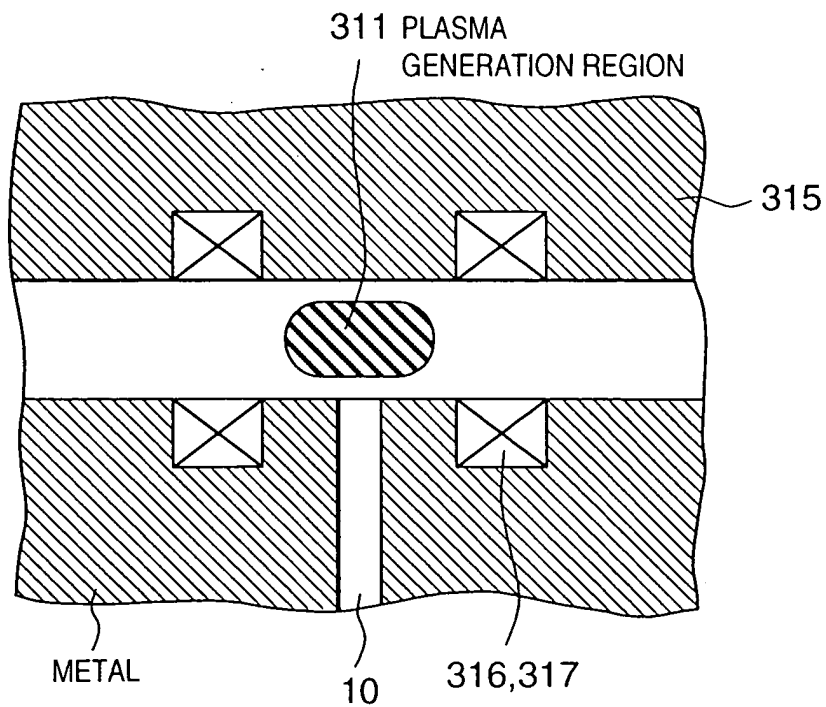


FIG. 39

NOZZLE SLOT-MAGNETIC FIELD COMPOSITE
TYPE CONFINING STRUCTURE

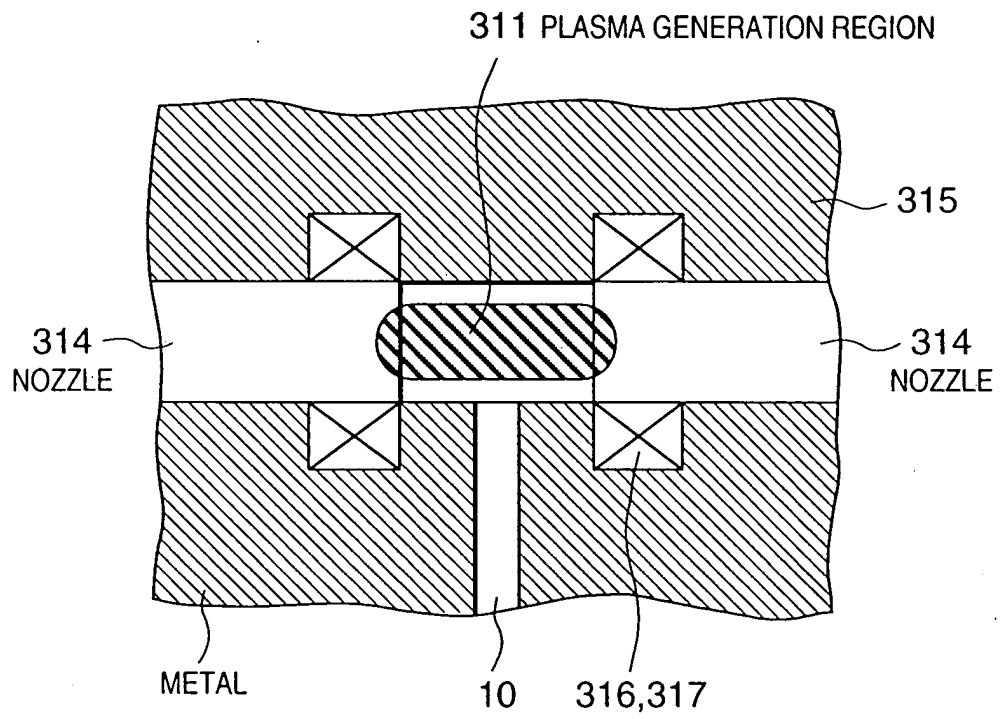


FIG. 40

WHEN SLOT WIDTH IS SMALL

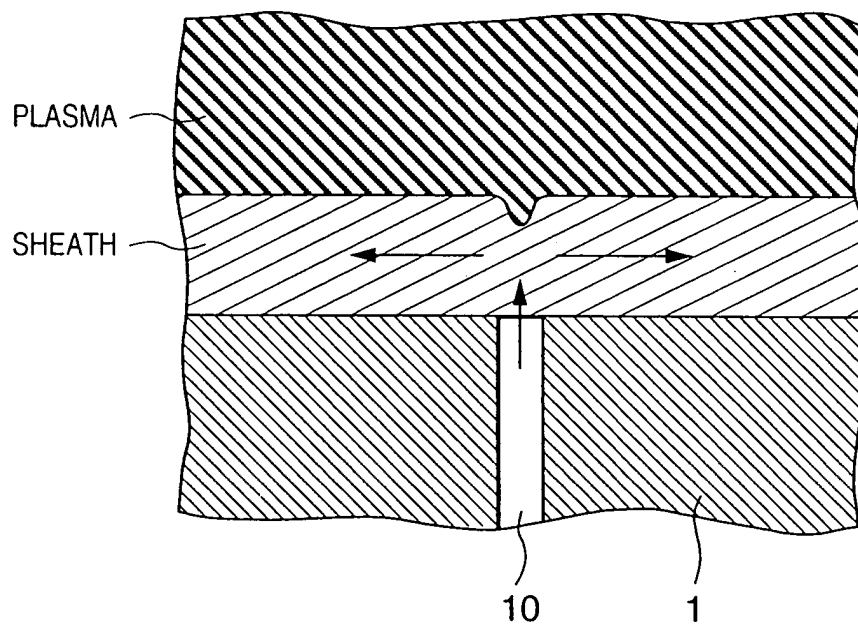


FIG. 41

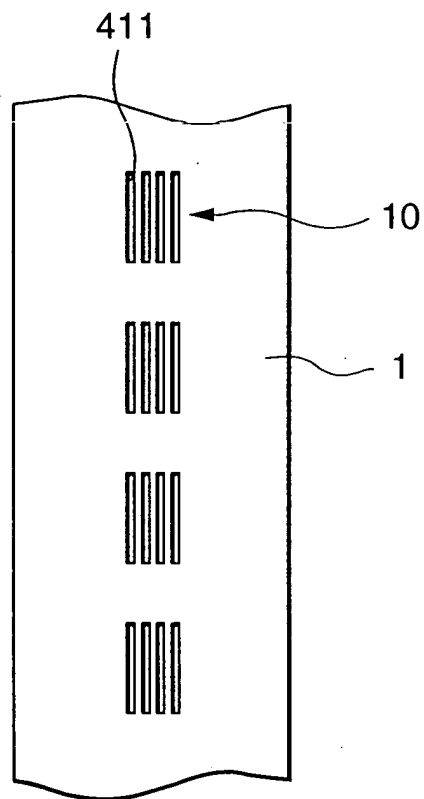
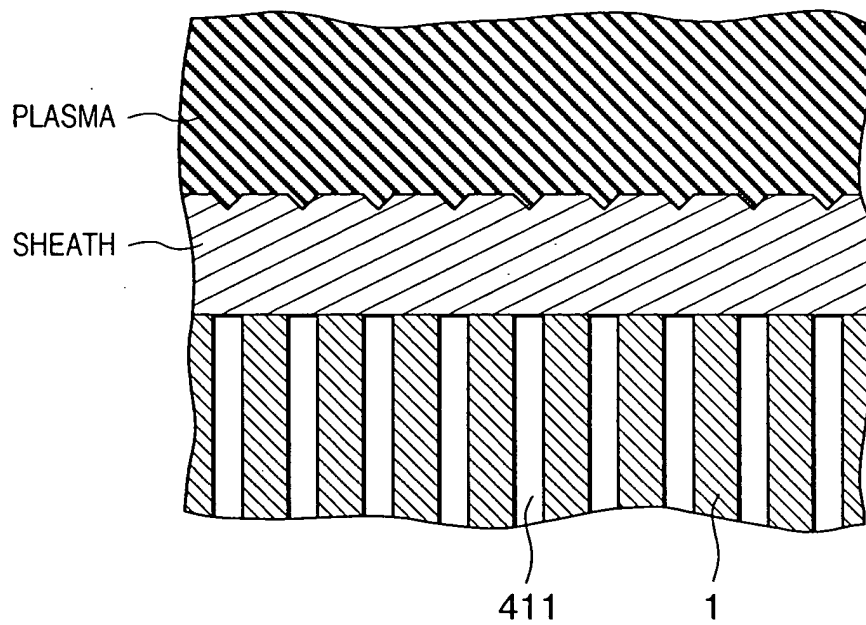


FIG. 42

WHEN SLOT WIDTH IS SMALL



007020" 5454460

FIG. 43

WHEN SLOT WIDTH IS SMALL

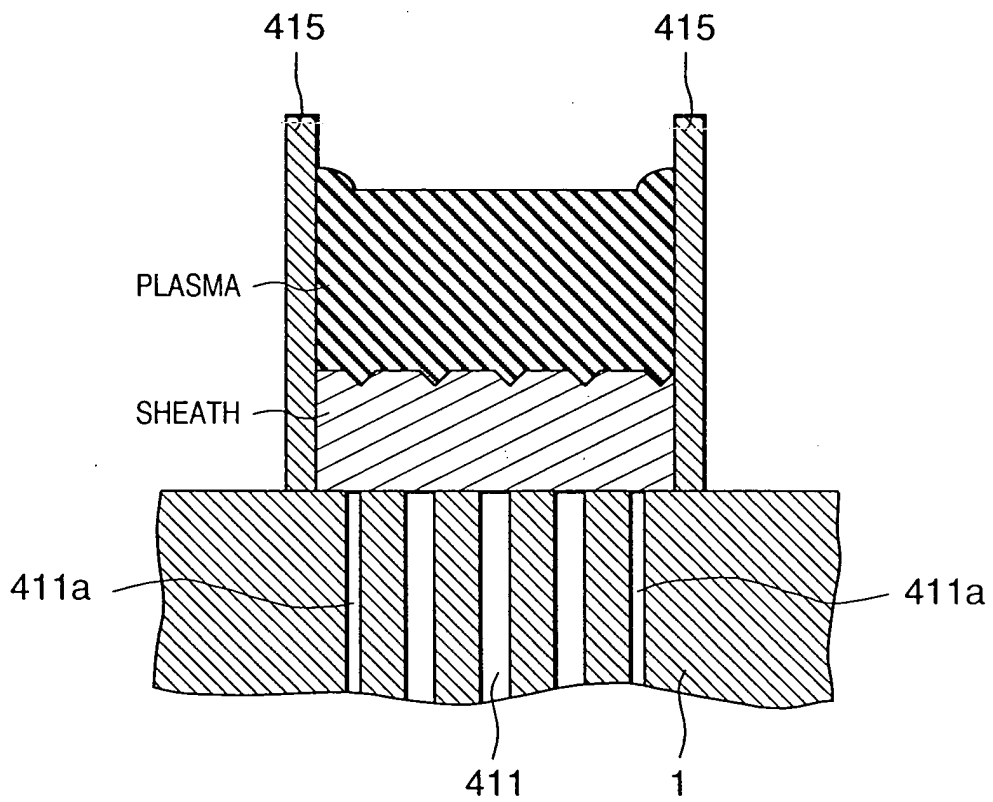


FIG. 44

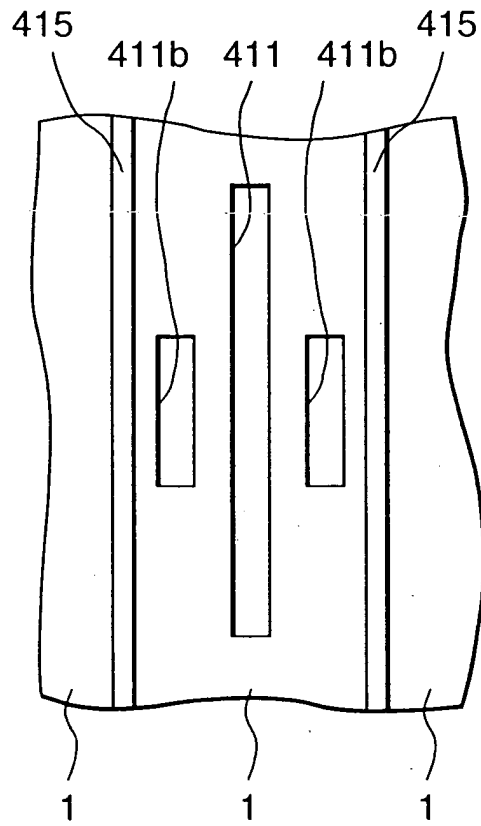


FIG. 45

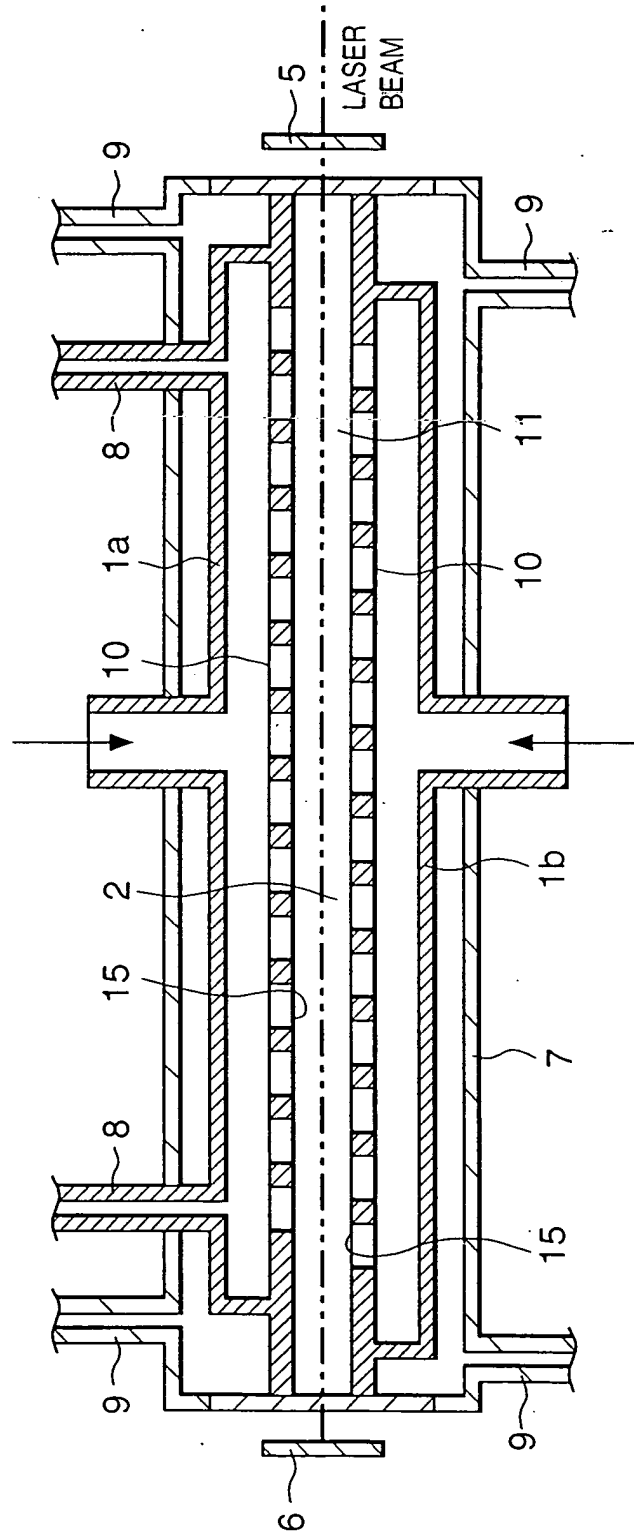


FIG. 46

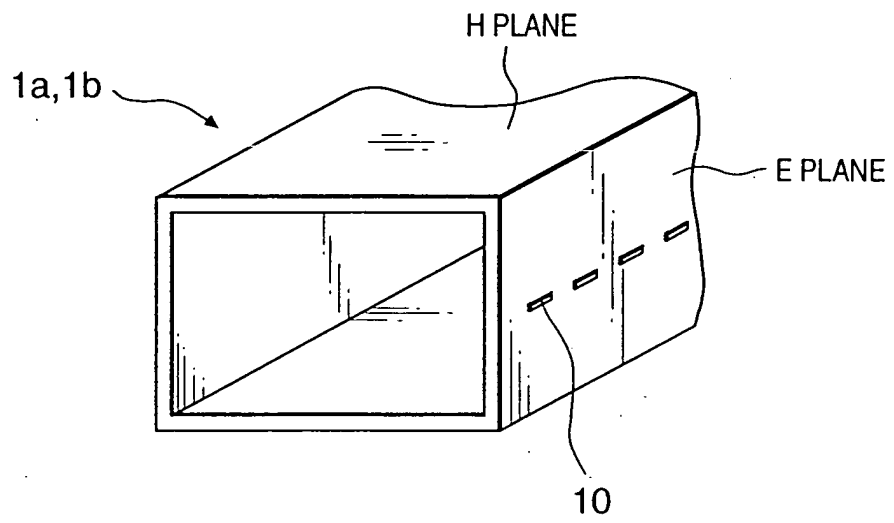


FIG. 47

RELATIVE POSITION TO
NORMAL WAVEGUIDE END $1/\lambda g$

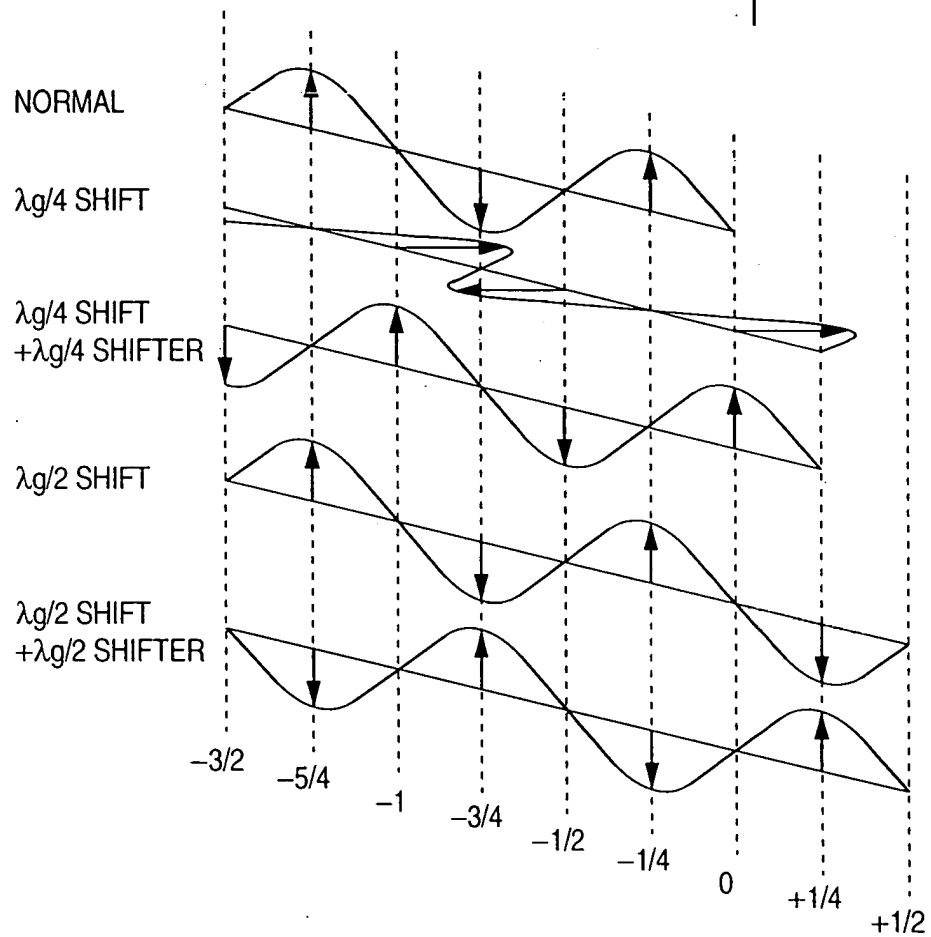
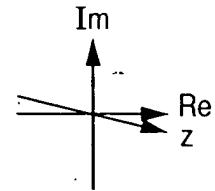
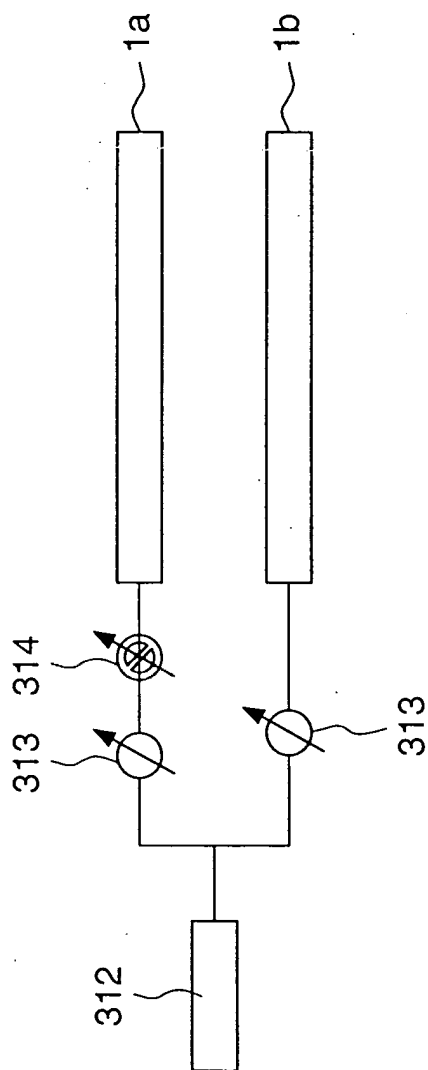


FIG. 48



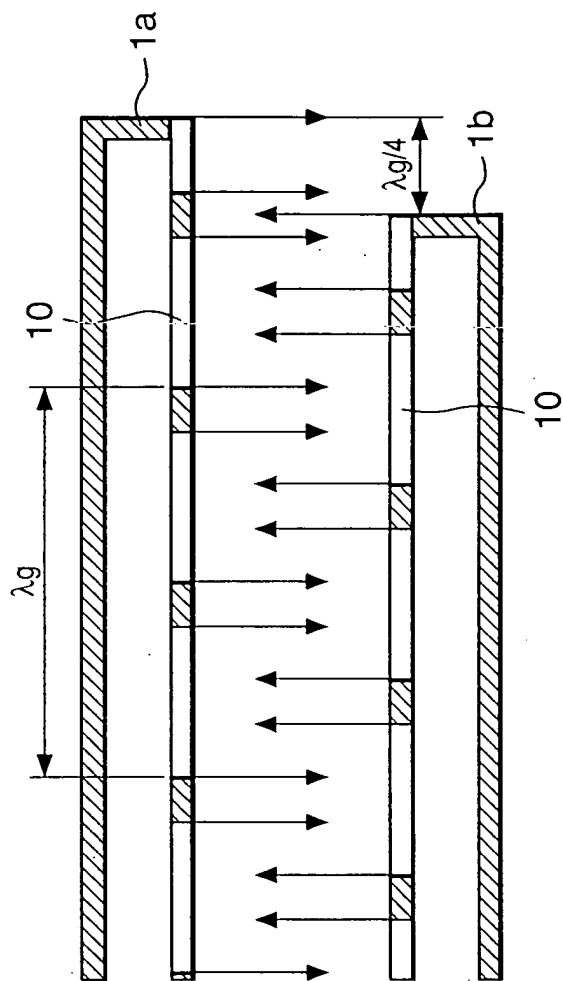


FIG. 49A

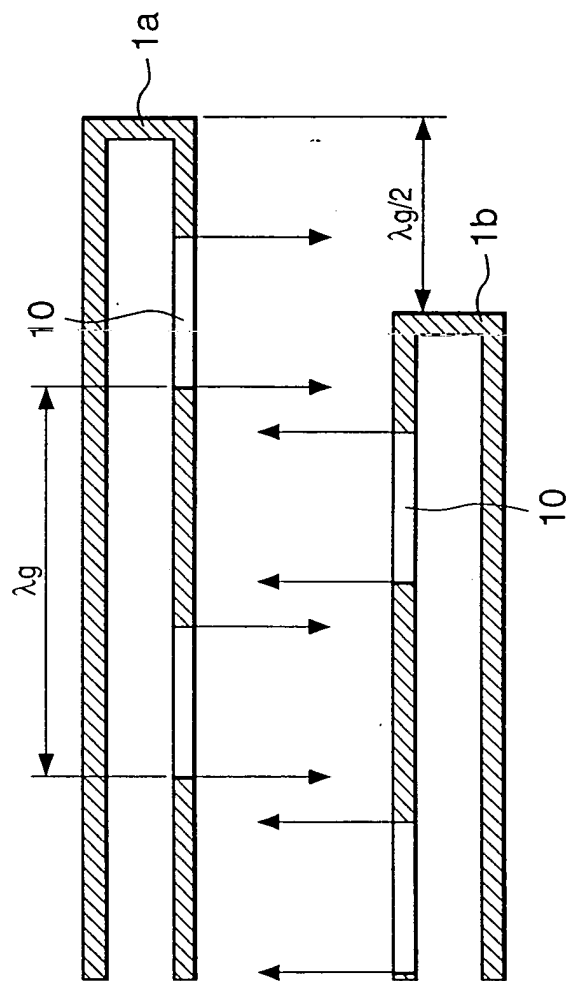


FIG. 49B

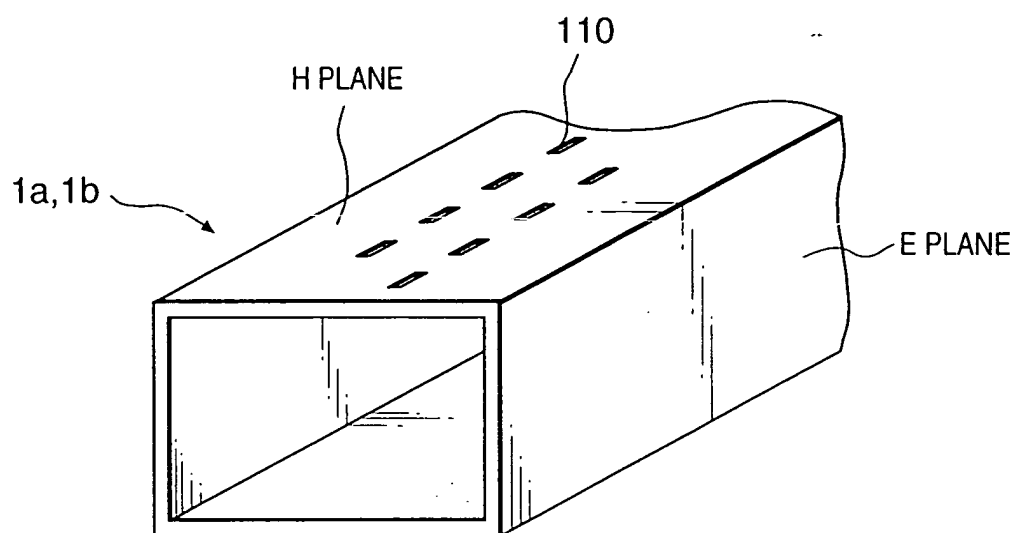
FIG. 50

FIG. 51

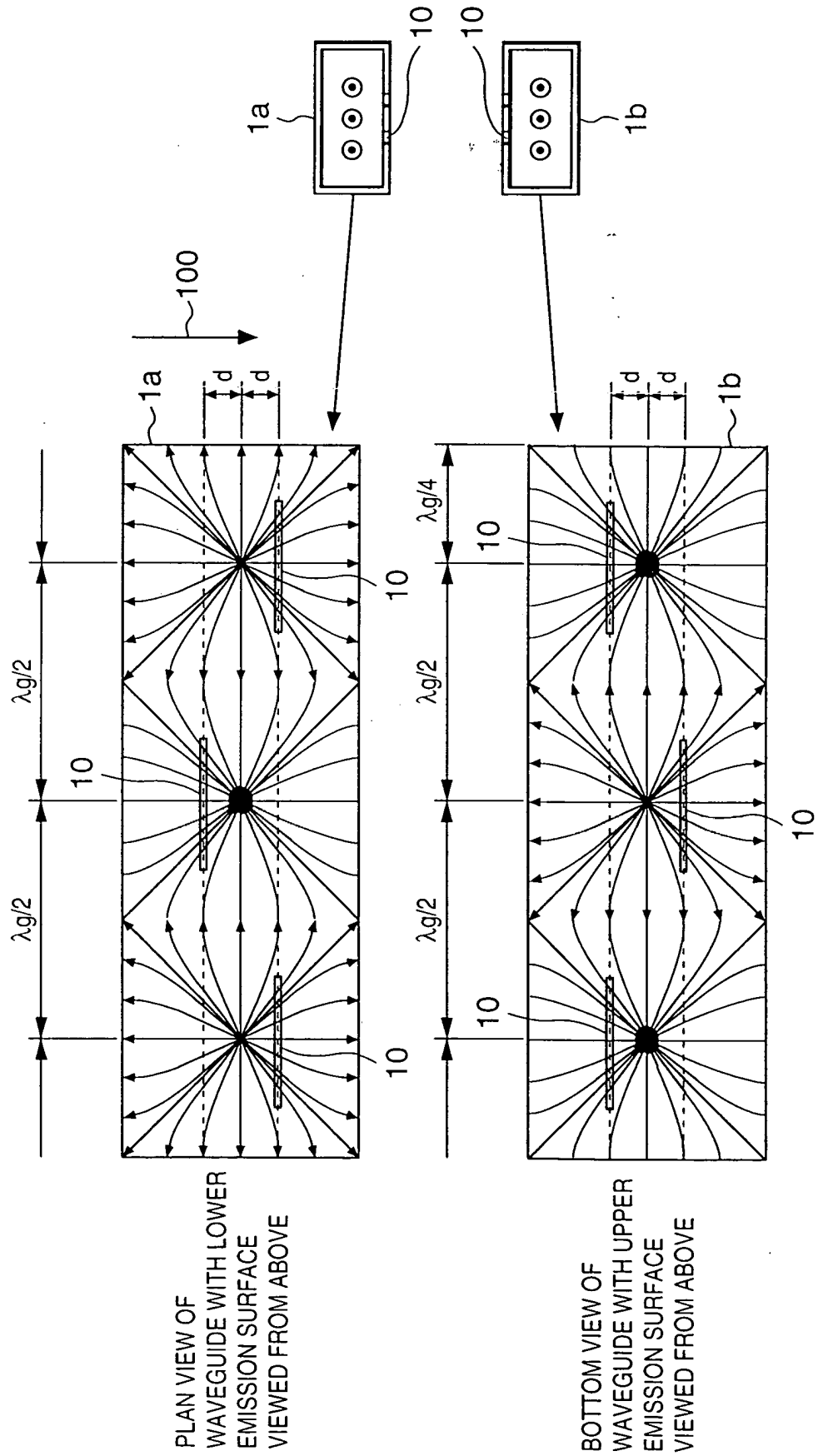


FIG. 53

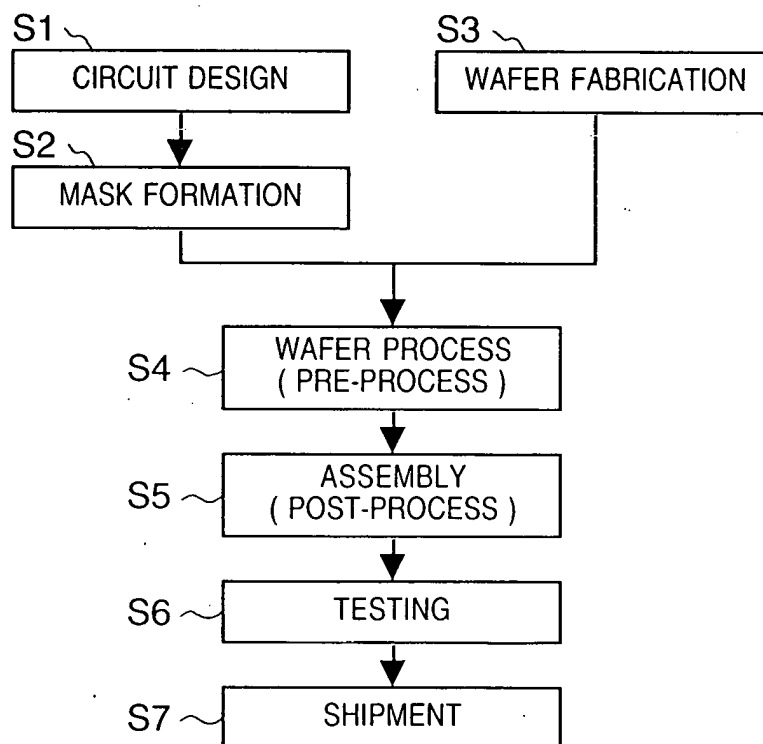


FIG. 54

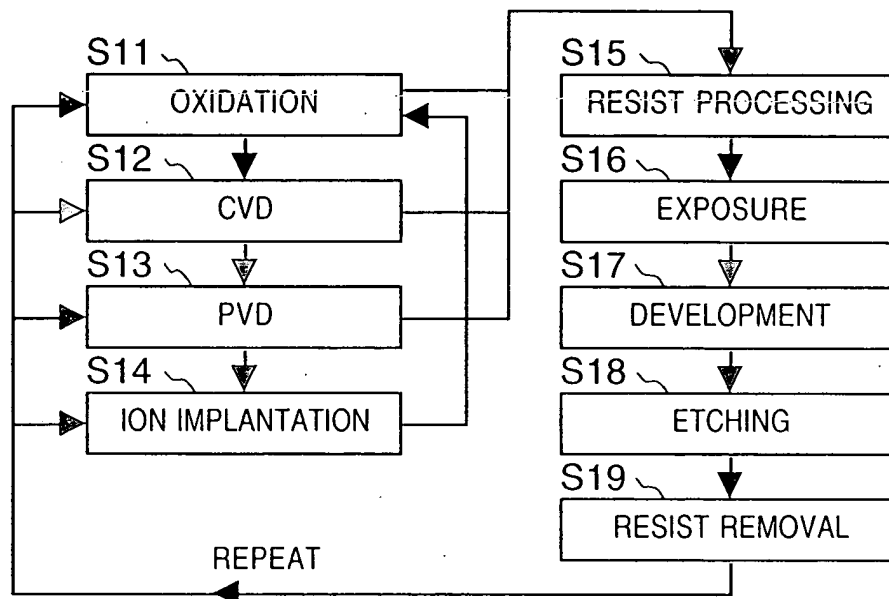


FIG. 55

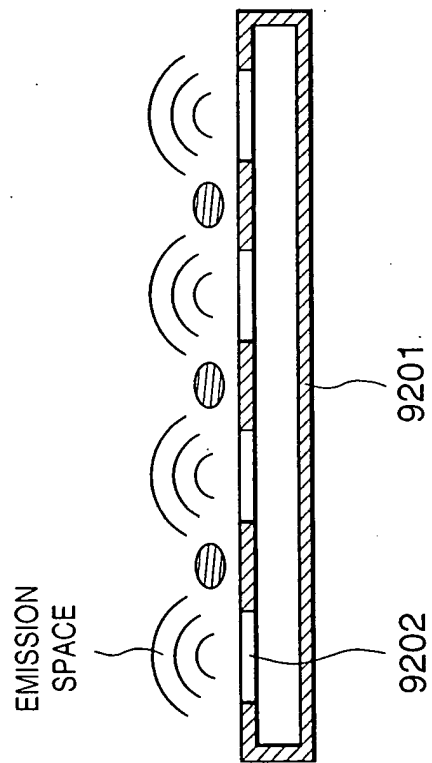


FIG. 56A

EXAMPLE OF ELECTRIC FIELD
INTENSITY NEAR SLOT

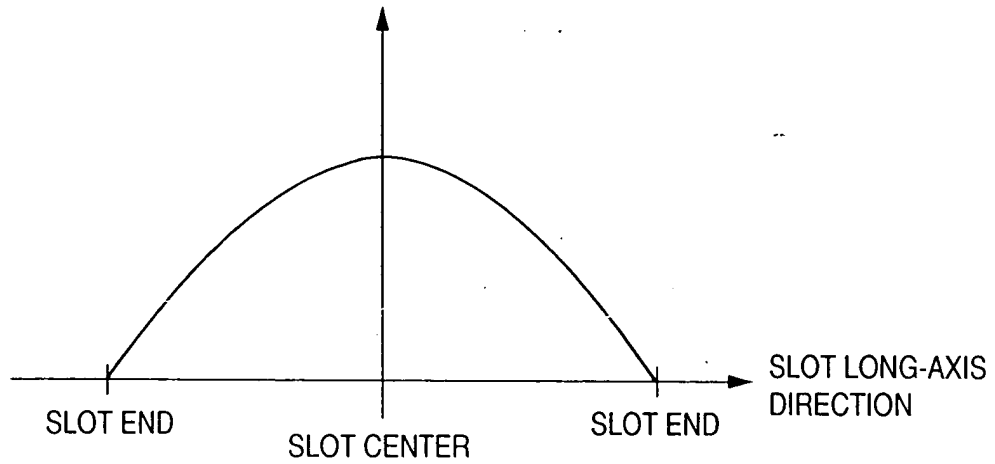


FIG. 56B

PLASMA WAVE INTENSITY
(ALONE)

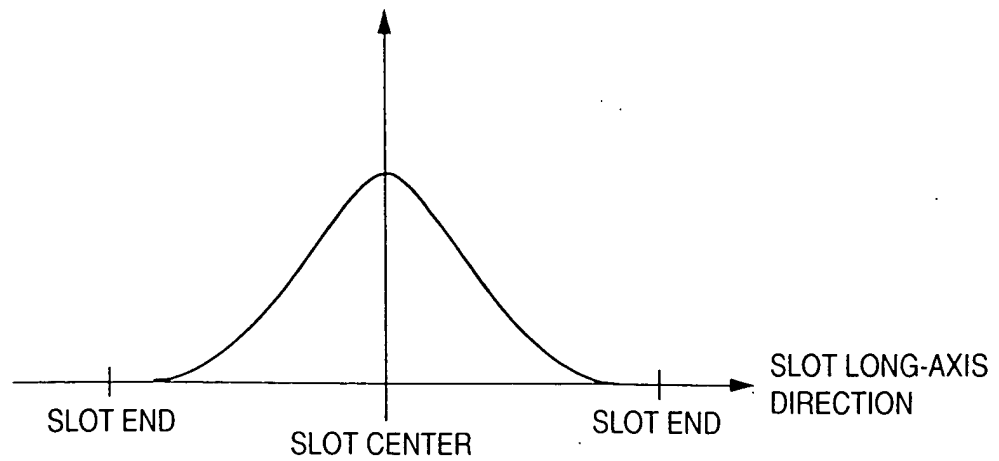


FIG. 57

